ChemBioEng Reviews

Check for updates

Catalytic Biomass Gasification in Supercritical Water and Product Gas Upgrading

Athanasios A. Vadarlis[1,*], Sofia D. Angeli[2], Angeliki A. Lemonidou[3,4], Nikolaos Boukis[1], Jörg Sauer[1]

Abstract

The gasification of biomass with supercritical water, also known as SCWG, is a sustainable method of hydrogen production. The process produces a mixture of hydrogen, carbon oxides, and hydrocarbons. Upgrading this mixture through steam or dry reforming of hydrocarbons to create synthesis gas and then extra hydrogen is a viable way to increase hydrogen production from biomass. This literature review discusses combining these two processes and recent experimental work on catalytic SCWG of biomass and its model compounds and steam/dry reforming of produced hydrocarbons. It focuses on catalysts used in these processes and their key criteria, such as activity, selectivity towards hydrogen and methane, and ability to inhibit carbon formation and deposition. A new criterion is proposed to evaluate catalyst performance in biomass SCWG and the need for further upgrading via reforming, based on the ratio of hydrogen bound in hydrocarbons to total hydrogen produced during SCWG. The review concludes that most catalysts used in biomass SCWG trap a large proportion of hydrogen in hydrocarbons, necessitating further processing of the product stream.

Keywords: Catalytic biomass gasification, Hydrocarbons, Product gas upgrading, Steam/dry reforming, Supercritical water gasification

Received: January 31, 2023; *revised:* April 21, 2023; *accepted:* June 02, 2023

DOI: 10.1002/cben.202300007

This is an open access article under the terms of the Creative Commons Attribution License, which permits use, distribution and reproduction in any medium, provided the original work is properly cited.

1 Introduction

Climate change is considered one of the greatest threats to the future life of humans and other living organisms [1]. Rising global temperature drastically affects climate change and its levels have increased rapidly due to human activities specifically related to energy and industrial sectors. Until now, most of the energy and the products needed in daily human lives come from fossil sources, which have generated enough carbon dioxide to significantly affect this rise in global temperature. On December 2015 in Paris, the World Climate Summit set the goal to reduce the emission of greenhouse gases and especially of CO_2 to net-zero by 2050 and to 50 % by 2030 [1–3]. To achieve this, the decarbonization of the energy sector and of the chemical industry is necessary. A promising step towards this goal is an energy transition based on various technologies for the production and use of hydrogen [4, 5]. The importance of hydrogen is high, as in addition to its crucial role as raw material and intermediate product for the production of many important chemicals, such as ammonia and synthetic fuels, in a powerful energy carrier with combustion free of harmful carbon oxides [1].

Until today, hydrogen production is based mostly on the utilization of fossil fuels [1]. Instead, renewable energy resources must be utilized, one of them being biomass. Biomass originates from many resources mostly agricultural, municipal, and animal [6]. Depending on its origin the composition may be different with the most important categories being the oil-based and lignocellulosic biomass. The model compounds of the latter are the monomers that result from the breakdown of

[1] Athanasios A. Vadarlis https://orcid.org/0009-0000-3209-7896 (athanasios.vadarlis@kit.edu),
Dr. Nikolaos Boukis, Prof. Dr.-Ing. Jörg Sauer
Karlsruhe Institute of Technology (KIT), Institute of Catalysis Research and Technology (IKFT), Hermann-von-Helmholtz-Platz 1, 76344 Eggenstein-Leopoldshafen, Germany.

[2] Dr.-Ing. Sofia D. Angeli
Karlsruhe Institute of Technology (KIT), Institute for Chemical Technology and Polymer Chemistry (ITCP), Engesserstr. 18/20, 76131 Karlsruhe, Germany.

[3] Prof. Dr. Angeliki A. Lemonidou
Aristotle University of Thessaloniki (AUTH), Department of Chemical Engineering, University Campus, 54124 Thessaloniki, Greece.

[4] Prof. Dr. Angeliki A. Lemonidou
Chemical Process Engineering Research Institute (CERTH/CPERI), P.O. Box 6036, Thermi, Thessaloniki, 57001, Greece.

macromolecules that make up the biomass resources, e.g., glucose that originates from cellulose.

A technology that utilizes biomass for hydrogen production is the gasification with water under supercritical conditions, referred to as SCWG. This technology developed in the 1970s has gained a lot of scientific interest since then [7]. Under supercritical conditions, i.e., $T > 374\,°C$ and $p > 221$ bar, the density of water, its viscosity, ion dissociation constant, and dielectric constant decrease dramatically in comparison with its values under near critical conditions. This leads to a drastic decrease of its inorganic solubility and a significant increase of its solubility in nonpolar substances [7].

Under noncritical conditions, the nonpolar compounds would remain undissolved and could result in char and tar formation. In addition, the low viscosity enhances the diffusivity of the reactants, leading in turn to higher reaction rates [8]. In the presence of supercritical water, biomass long-chain molecules undergo hydrolysis and are converted into their respective monomers [7]. The main chemical reactions that govern the process of SCWG can be divided into three main categories. The first category contains the reactions of the biomass monomers and/or their pseudo-components with supercritical water to form hydrogen and carbon oxides [9]:

$$C_xH_yO_z + (2x - z)H_2O \rightarrow xCO_2 + \left(2x - z + \frac{y}{2}\right)H_2 \quad (1)$$

$$C_xH_yO_z + (x - z)H_2O \rightarrow xCO + \left(x - z + \frac{y}{2}\right)H_2 \quad (2)$$

The second category contains the reactions that involve the gas products from the steam reforming reactions, the methanation reaction of CO (Eq. (3)) and the WGS, which stands for water-gas shift (WGS; Eq. (4)):

$$CO + 3H_2 \rightleftharpoons CH_4 + H_2O \quad \Delta H^{298K} = -206 \text{ kJ mol}^{-1} \quad (3)$$

$$CO + H_2O \rightleftharpoons CO_2 + H_2 \quad \Delta H^{298K} = -41.2 \text{ kJ mol}^{-1} \quad (4)$$

The third category is related to all the reactions that lead to tars formation, e.g., dehydration and condensation reactions [10, 11] and to coke formation, i.e., coke from intermediates decomposition (Eq. (5)), CO reduction (Eq. (6)), Boudouard reaction (Eq. (7)) and CH_4 decomposition (Eq. (8)) [7, 12]:

$$C_xH_yO_z \rightarrow \text{Coke} \quad (5)$$

$$CO + H_2 \rightleftharpoons C + H_2O \quad \Delta H^{298K} = -131 \text{ kJ mol}^{-1} \quad (6)$$

$$2CO \rightleftharpoons C + CO_2 \quad \Delta H^{298K} = -172 \text{ kJ mol}^{-1} \quad (7)$$

$$CH_4 \rightleftharpoons C + 2H_2 \quad \Delta H^{298K} = 75 \text{ kJ mol}^{-1} \quad (8)$$

The SCWG of organic substances involves reactions such as water-gas shift and methanation, which have high activation energies and therefore need a catalyst [8, 9, 11, 13–15]. Apart from that it has been shown that catalysts can enhance carbon gasification efficiency and facilitate the approach to equilibrium gas yield [14, 16]. Ni-based catalysts, e.g., favor the cleavage of C–C bonds instead of dehydration and condensation reactions, inhibiting therefore tars formation [15]. Apart from the heterogeneous catalysts, homogeneous ones based on alkali metals, e.g., KOH, $KHCO_3$, K_2CO_3, and $Ca(OH)_2$, have been shown to promote hydrogen and carbon dioxide production [7–9]. Their main disadvantage is that they are difficult to recover from the output of the system and therefore a new batch of catalyst is required for each new feed. In addition, the inner surface of the reactor can act as a catalyst for the SCWG of organic solutions [17].

Elliot and his group contributed significantly to the early development of the catalytic hydrothermal gasification of biomass [18]. They designed and patented Ni-based catalysts with various metal promoters, facing the problems related with the loss of activity, i.e., crystallite sintering and support breakdown [19, 20]. These authors were also among the first who worked with continuous-flow gasification of biomass and addressed the problems that are associated with its utilization, like reactor plugging [20, 21]. Vogel et al. contributed significantly to the field of hydrothermal processing of biomass. Apart from investigating the performances of Ni-based catalysts supported on α-alumina, they experimented on Raney-Ni catalysts and Ru/C as well [21–24]. The work of Vogel et al. on process development for the catalytic hydrothermal gasification [25, 26], on salt separation [27–29], and on the parameters that affect mostly coke and tar formation [30], is also remarkable.

Correa and Kruse [8] summarized in their review the recent progress in SCWG of biomass for hydrogen production, categorizing the main factors that affect it. The same topic was investigated by Ferreira-Pinto et al. [7] for simple organic matter like ethanol and cellulose, and Lee et al. [9] for real biomass, including both the thermodynamics of this process, reaction mechanisms, and aspects of materials corrosion.

The SCWG of biomass generates a product gas that consists of H_2, CH_4, CO_2, CO, and other hydrocarbons, mainly C_2–C_3. Part of the hydrogen produced is bound in the hydrocarbons formed. In order to maximize pure hydrogen gas, a downstream upgrading process is necessary, which will transform the bound hydrogen into molecular hydrogen. In their recemt publication, Boukis and Stoll [31] described the work that has been done at the Karlsruhe Institute of Technology (KIT) regarding the SCWG of biomass in lab-scale and in a pilot plant-scale unit called "VERENA". They reported that to result with pure hydrogen in the product stream, a reforming step of the produced hydrocarbons is required. Azadi and Farnood [32] mentioned a sequence of two steps including steam reforming and WGS following the catalytic SCWG of organic feed.

Steam methane reforming, generally known as SMR, is the most common technology used for the production of hydrogen [33]. A methane source, e.g., natural gas or biogas, is utilized and reacts with steam at ratios of steam/CH_4 = 2.5–3 under temperature ranging from 700 to 1000 °C and a pressure range of 3–30 bar [33–35]. The main reaction of this process, which is the reverse reaction of Eq. (3), involving as co-reactants methane and steam is highly endothermic [36]. A side reaction, which takes place and is of high importance, is the WGS reaction (Eq. (4)). If the feed consists also of hydrocarbons higher than methane, their steam reforming reactions and their decomposition should be also taken into consideration:

 © 2023 The Authors. ChemBioEng Reviews published by Wiley-VCH GmbH

21969744, 0, Downloaded from https://onlinelibrary.wiley.com/doi/10.1002/cben.202300007 by Karlsruher Institution F. Technologie, Wiley Online Library on [26/07/2023]. See the Terms and Conditions (https://onlinelibrary.wiley.com/terms-and-conditions) on Wiley Online Library for rules of use; OA articles are governed by the applicable Creative Commons License

$$C_nH_m + H_2O \rightarrow nCO + \left(\frac{m}{2} + n\right)H_2 \quad (9)$$

$$C_nH_m \rightarrow nC + \frac{m}{2}H_2 \quad (10)$$

The aforementioned side reactions that generate coke, i.e., CO reduction, Boudouard, and the decomposition of methane also take place in the methane reforming process. A conventional SMR process operates in the presence of a nickel catalyst and produces syngas with a H_2/CO ratio of around 3.

Dry reforming of methane, referred to as DRM, has also gained a lot of scientific interest in the last decades. This process is preferred when the feed consists of a significant amount of CO_2, e.g., biogas. DRM typically produces syngas with H_2/CO ratio of unity, which can be utilized in the production of higher hydrocarbons via the Fischer-Tropsch synthesis [37]. The DRM main reaction that is also highly endothermic is the following:

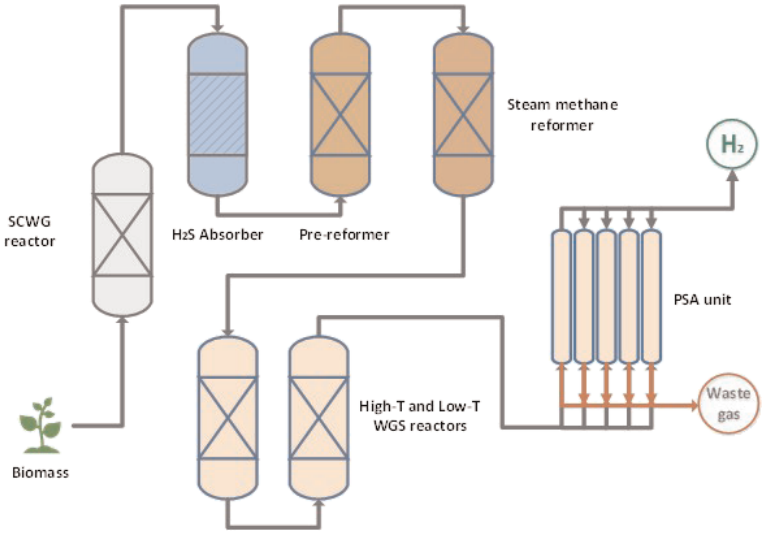

Figure 1. Simplified process diagram for the hydrogen production from biomass resources via supercritical water gasification and sequential reforming of the generated hydrocarbons.

$$CH_4 + CO_2 \rightleftharpoons 2CO + 2H_2 \quad \Delta H^{298K} = 247 \text{ kJ mol}^{-1} \quad (11)$$

When CO_2 and H_2O are both implemented as reactants, under certain conditions, a combined steam and dry reforming of methane takes place, which can be called bireforming, also known as BRM [35].

LeValley et al. [38] presented the progress in steam reforming catalysts for hydrogen production. Angeli et al. [33] critically reviewed the progress on catalysts for methane steam reforming at low temperatures. Abdullah et al. [37] reviewed the advances of Ni-based catalysts for DRM. Recently, Mohanty et al. [3] discussed the progress on catalysts used at BRM for syngas production. Catalyst development for biogas dry, bi-and tri-reforming, i.e., steam reforming, dry reforming, and partial oxidation, has been also reviewed [39, 40]. Another review article focusing on the main factors of catalyst design, such as active metal size, promoters, support etc., that affect their performance in SMR applications was recently published [34]. Another team of researchers [41] reviewed novel Ni-based catalysts, their production methods, and the innovative structures of their carriers.

To the best of the authors' knowledge, there has not been any literature specifically for the combination of the SCWG of biomass and the sequential reforming of the produced hydrocarbons. A simplified process flow diagram addressing this novel concept is illustrated in Fig. 1. Biomass is gasified with supercritical water in the first reactor. The product gas must be purified from poisonous compounds like H_2S, HCl, and COS, which contaminate the catalysts and inhibit steam reforming. Catalysts and adsorbents for this purpose are metal oxides of ZnO, CuO, Cr_2O_3, Al_2O_3 [42, 43]. After the cleaning step, a prereformer converts all the hydrocarbons higher than methane to H_2, CO, CO_2, and CH_4 [43]. The methane steam reformer is located downstream of the prereformer and converts the reactants into syngas.

Fig. 2 illustrates the classification of metal catalysts that can be used for the SCWG of biomass and for the reforming of methane and other hydrocarbons. The syngas is then converted via the WGS reaction to H_2 and CO_2. The last step of the process scheme is the purification of H_2 which is usually carried out in a pressure-swing adsorption (PSA) unit [44].

These two processes, if combined, provide an alternative technology for syngas and especially for hydrogen production based on renewable resources. There are many issues to consider when designing such a tandem process scheme, one of which is the selection of suitable catalysts and their supporting materials for SCWG of biomass and steam/dry reforming of hydrocarbons, which constitutes the aim of the present review.

The efficiency of processes like SCWG and SMR strongly depends on the catalysts, which can become deactivated due to various factors such as poisoning, fouling, thermal or chemical degradation, and mechanical failure [45]. Deactivating agents in SCWG mainly include sulfur, carbon deposition, salts, tars, and sintering of active metals [32, 46–48]. In SMR, the main causes of catalyst deactivation are carbon deposition, sulfur poisoning, and sintering [49, 50]. The disposal of those catalysts can be a serious threat to the environment. The metals that are present in the catalysts (e.g., Ni, Pt, Co, Pd, Rh) can be drained away by water and reach various environmental compartments posing a threat to plant and animal life or produce toxic gases such as HCN [51–53].

To address this issue in an environmentally and economically sustainable manner, it is important to consider the recovery and reuse of the deactivated catalysts [47, 54]. Several techniques have been developed and others are under investigation for dealing with the recovery of the deactivated SMR and SCWG catalysts. Generally, the carbon formed on catalysts can be gasified with steam, oxygen, carbon dioxide, and hydrogen [50]. Oxygen provides higher gasification rates than the other

 © 2023 The Authors. ChemBioEng Reviews published by Wiley-VCH GmbH

21969744, 0, Downloaded from https://onlinelibrary.wiley.com/doi/10.1002/cben.202300007 by Karlsruher Institution F. Technologie, Wiley Online Library on [26/07/2023]. See the Terms and Conditions (https://onlinelibrary.wiley.com/terms-and-conditions) on Wiley Online Library for rules of use; OA articles are governed by the applicable Creative Commons License

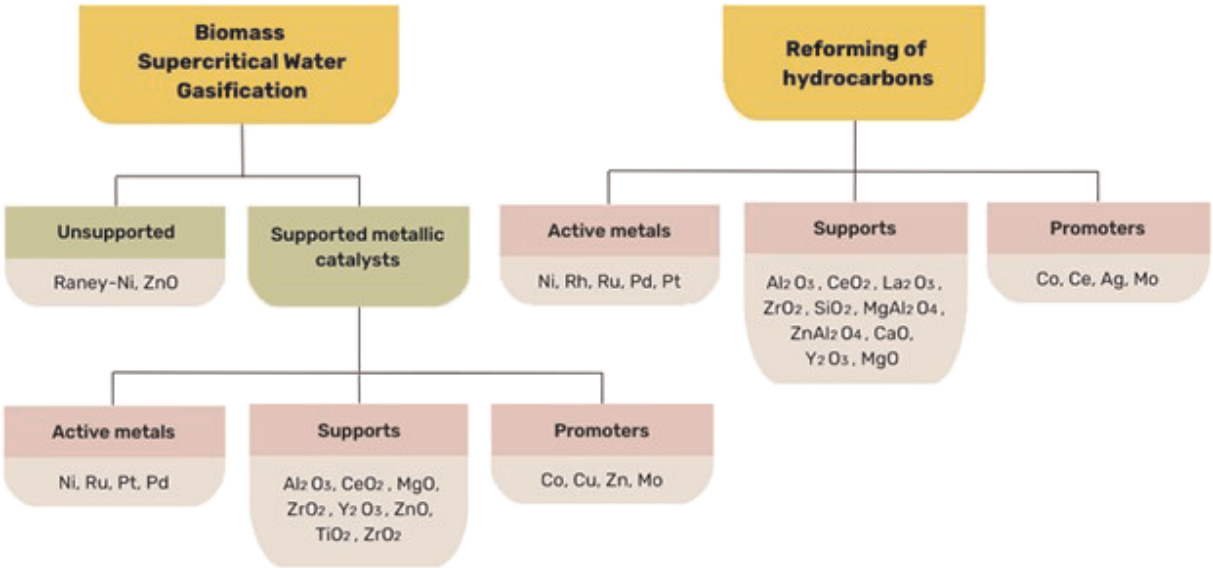

Figure 2. Classification of the metallic catalysts used in SCWG of biomass and reforming of the produced hydrocarbons.

gases, and thus, air is typically utilized at moderate temperatures, e.g., 400–600 °C [49]. Sulfur-poisoned catalysts are treated with oxygen/air, steam, hydrogen, and mixtures thereof [49, 50].

Using H_2O_2 has also been proven effective for sulfur removal in SCWG catalysts [46, 55]. In the catalytic reforming of hydrocarbons on platinum-containing catalysts, sintering can be dealt with by treating the used catalyst in oxygen and chlorine under high temperatures [49]. Ni-based catalysts for SMR that suffer from sintering can be redispersed with a mixture of CO_2, H_2O, and O_2 at 700 °C [50].

2 Catalysts for Supercritical Water Gasification of Organic Species

This chapter focuses on recent developments in catalysts for the supercritical water gasification of biomass and its model compounds. Two main criteria, namely, the carbon gasification efficiency (CGE) and the yield of the produced gases, are utilized for evaluating the performance of the catalysts.

The CGE is defined as the degree of conversion of carbon, which is contained in the organic feed, towards the product gases that contain it, i.e., CH_4, other hydrocarbons, CO, and CO_2:

$$\mathrm{CGE}\ (\%) = \frac{n_{\mathrm{C\ in\ product\ gas}}}{n_{\mathrm{C,feed}}} \tag{12}$$

The best case for the SCWG is to attain complete gasification of the organic feed. In this case, all the carbon that is present in the organic feed can be found in the product gases. However, this is an unrealistic scenario and, especially when real biomass is used as feedstock, the CGE is a matter of optimization. In most of cases, a relatively high CGE is found when not only H_2, CO_2, and CO, are produced but also CH_4 and other hydrocarbons, from Eqs. (3)–(5). In addition to CGE, the yields of H_2, CH_4, and total gas products are used in the discussion to compare the activities of the studied catalysts:

$$Y_{\mathrm{i}}(\mathrm{mol\ kg^{-1}}) = \frac{n_{\mathrm{i}}}{m_{\mathrm{feed}}}, \quad i = \mathrm{H_2\ or\ CH_4} \tag{13}$$

If the yields of all produced gases are added together, the total gas yield can be calculated as:

$$Y_{\mathrm{total}}(\mathrm{mol\ kg^{-1}}) = \frac{n_{\mathrm{H_2}} + n_{\mathrm{CH_4}} + n_{\mathrm{CO}} + n_{\mathrm{CO_2}} + n_{\mathrm{C_{2+}}}}{m_{\mathrm{feed}}} \tag{14}$$

Focus has been given on the catalysts that consist of a transition metal as the catalytically active phase and one or more metal oxides as the support. The catalysts are classified based on the supports, as their role is important both in the gasification and in reforming. A summary table, i.e., Tab. 1, of the catalysts discussed in the main text is provided. This table contains the catalysts from the most representative sources. In this table, a new evaluation criterion is introduced expressing the quantity of hydrogen produced bound in methane and other hydrocarbons versus the total quantity of hydrogen in the products including the diatomic hydrogen:

$$R_{\mathrm{Hydrogen\ bound}} = R_{\mathrm{Hb}} = \frac{n_{\mathrm{Hydrogen\ in\ hydrocarbons}}}{n_{\mathrm{Hydrogen\ in\ hydrocarbons}} + 2n_{\mathrm{H_2}}} \tag{15}$$

This parameter in combination with CGE indicates if the gas produced needs to be upgraded with a subsequent reforming process towards additional syngas production.

2.1 Catalysts Based on Al_2O_3

Azadi et al. [56] tested Ni-based catalysts (5 wt % Ni) with a variety of different supports for SCWG of a 2 wt % glucose-

 © 2023 The Authors. ChemBioEng Reviews published by Wiley-VCH GmbH

21969744, 0, Downloaded from https://onlinelibrary.wiley.com/doi/10.1002/cben.202300007 by Karlsruher Institution F. Technologie, Wiley Online Library on [26/07/2023]. See the Terms and Conditions (https://onlinelibrary.wiley.com/terms-and-conditions) on Wiley Online Library for rules of use; OA articles are governed by the applicable Creative Commons License

Table 1. Catalysts for SCWG of organic feedstock and their activity in terms of CGE and H_2 gas yield. The ratio R_{Hb} is also given to show how much of the produced hydrogen is bound to the hydrocarbons. The conditions to which each catalyst was subjected are also recorded, i.e. temperature, pressure, feed and residence time or space velocity, for batch or continuous processes respectively.

Catalyst	Feed	Temp. T [°C]	Pressure p [bar]	Space velocity [h^{-1}]	Reaction time [h]	CGE [%]	H_2 yield [mol kg_{feed}^{-1}]	R_{Hb} [%]	Ref.
I)	*Catalysts supported on Al_2O_3 and Raney-Ni catalysts*								
Ni(4wt %)-Mo(21wt %)/Al_2O_3	*C. vulgaris* (7.3wt %)	600	240	–	0.033	62	–	73.33	[14]
Pt(0.63wt %)-Pd(0.68wt %)/Al_2O_3	*C. vulgaris* (7.3wt %)	600	240	–	0.033	65.8	–	83.02	[14]
Co(5wt %)-Mo(20wt %)/Al_2O_3	*C. vulgaris* (7.3wt %)	600	240	–	0.033	64	–	87.24	[14]
Ni(65wt %)/Al_2O_3-SiO_2	Primary paper water sludge (10wt %)	450	292	–	2	85.9	6	84.01	[16]
Raney-Ni (50wt % solid catalyst – 50 wt % water)	Sugarcane bagasse (9wt %)	400	250	–	1.25	53.1	1.3	94.12	[11]
Ru-Ni(10wt %)/γ-Al_2O_3 (Ru/Ni molar ratio = 0.1)	Glucose (5wt %)	600	240	6	–	99.2	25.5	34.25	[10]
	Glucose (5wt %)	750	240	6	–	99.6	53.9	5.38	[10]
Ni(5wt %)/α-Al_2O_3	Glucose (2wt %)	380	230	–	1	67	24.3	27.46	[56]
Ni(20wt %)-Cu(5wt %)/γ-Al_2O_3	Glucose (9wt %)	400	–	–	0.33	32.13	10.9	23.78	[61]
Ni(20wt %)-Co(5wt %)/γ-Al_2O_3	Glucose (9wt %)	400	–	–	0.33	21.02	8.5	19.05	[61]
Ni(20wt %)-Sn(5wt %)/γ-Al_2O_3	Glucose (9wt %)	400	–	–	0.33	21.02	3.95	33.61	[61]
Ni(10wt %)-Co(6wt %)/Al_2O_3	Cellulose (1.6 wt %)	350	165–180	–	0.33	55.08	59	10.06	[62]
Ru(5wt %)/α-Al_2O_3	Glucose (5wt %)	550	360	–	0.166	96.2	10	62.70	[71]
	Cellulose (5wt %)	550	360	–	0.166	96.4	8.5	63.68	[71]
Ru(5wt %)/γ-Al_2O_3	Bagasse (1.25 wt %)	400	–	–	0.25	45	14	3.85	[74]
Ru(5wt %)-Zn(1.5wt %)/γ-Al_2O_3	Bagasse (1.25 wt %)	400	–	–	0.25	30	15.6	2.88	[74]
Ni(12wt %)/α-Al_2O_3	*C. vulgaris* (5wt %)	385	260	–	1.5	87	2.5	94.74	[75]
Raney-Ni(68.2wt %)	*C. vulgaris* (5wt %)	385	260	–	1.5	88	2.5	95.22	[75]
Raney-Ni(93.57wt %)-Mo(0.31wt %)	Sewage sludge (8.9wt %)	450	214–286	–	0.42	90.1	18.13	55.39	[78]
Ni(20wt %)-Ce/Al_2O_3 (Ce/Ni = 0.36, molar ratio)	Lignin (20wt%)	650	260	–	0.83	–	2.15	55.42	[65]
II)	*Catalysts supported on CeO_2 or CeO_2-Al_2O_3*								
Ni(10wt %)/CeO_2-Al_2O_3	Glucose (10wt %)	400	235	–	0.33	76.6	1	33.33	[66]
Ni(20wt %)/CeO_2-γ-Al_2O_3 (Ce: 5wt %)	Glucose (9.09wt %)	400	245	–	0.33	58.05	12.7	31.35	[79]
Ni(10wt %)/CeO_2-Al_2O_3	Glucose (12.5wt %)	400	–	–	0.5	10	0.85	39.29	[80]
Ni(20wt %)/CeO_2-Al_2O_3 (Ce = 8.46wt %)	Glucose (9.09wt %)	400	245	–	0.33	33.03	12.99	23.54	[81]

 © 2023 The Authors. ChemBioEng Reviews published by Wiley-VCH GmbH

21969744, 0, Downloaded from https://onlinelibrary.wiley.com/doi/10.1002/cben.202300007 by Karlsruher Institution F. Technologie, Wiley Online Library on [26/07/2023]. See the Terms and Conditions (https://onlinelibrary.wiley.com/terms-and-conditions) on Wiley Online Library for rules of use; OA articles are governed by the applicable Creative Commons License

Table 1. Continued.

Catalyst	Feed	Temp. T [°C]	Pressure p [bar]	Space velocity [h^{-1}]	Reaction time [h]	CGE [%]	H_2 yield [mol kg_{feed}^{-1}]	R_{Hb} [%]	Ref.
Ru(1wt %)/CeO_2	HTL[b)] downs. Water (no pure water added)	600	460–520	–	1	83.26	1.05	77.66	[82]
III)	*Catalysts supported on MgO or MgO-Al_2O_3*								
$Mg_{0.8}Ni_{0.2}O$	Oil palm frond (3wt %)	400	250	–	0.5	–	–	53.95	[84]
Ni(5wt %)/MgO	Glucose (2wt %)	380	230	–	1	72	26.9	31.55	[56]
Ni(2.6wt %)-Co(5.2wt %)/Mg-Al	Lignin (20wt %)	650	260	–	0.83	–	2.36	58.06	[58]
Ni(26.3wt %)/$MgAl_2O_4$-Al_2O_3	Glucose (5wt%)	400	221	–	0.33	70	11.8	57.55	[59]
Ni(28.6wt %)/$Mg_{0.6}$ –$Al_{1.9}$	Glucose (9wt %)	400	225–250	–	0.33	70	11.77	56.68	[63]
SG[a)]-Ni(30wt %)/MgO-Al_2O_3	Glycerol (20wt %)	500	230	–	0.33	68.3	6.52	74.47	[70]
SC[a)]-Ni(30wt %)/MgO-Al_2O_3	Glycerol (20wt %)	500	230	–	0.33	55.3	9.77	57.14	[70]
Ni(10wt %)/MgO	Glucose (12.5wt %)	400	–	–	0.5	–	0.8	39.39	[80]
Ru(1wt %)/MgO	HTL[b)] downs. water	600	460–520	–	1	71.46	0.79	78.24	[82]
IV)	*Catalysts supported on ZrO_2 or MgO-ZrO_2*								
Ni(10wt %)/ZrO_2	Soybean straw/water (1:10)	500	230–250	–	0.75	21.5	8.10	46.71	[57]
Ni(10wt %)-Ce(1wt %)/ZrO_2	Soybean straw/water (1:10)	500	230–250	–	0.75	33.5	10.90	47.09	[57]
Ni(15wt %)/ZrO_2	Polyethylene glycol (2 g L^{-1})	390	240	0.05	–	48.50	37.30	15.42	[89]
Ni(15wt %)-Co(5wt %)/ZrO_2	Polyethylene glycol (2 g L^{-1})	390	240	0.05	–	59	50	13.79	[89]
Ni/ZrO_2 (Ni/Zr molar ratio = 0.4:0.6)	Glycerol (20wt %)	500	230	–	0.5	93.8	4.78	53.19	[90]
Ni(20wt %)/MgO-ZrO_2	Glycerol (5wt %)	800	245	3600	–	95	70.58	17.72	[86]
	Glycerol (5wt %)	700	245	3600	–	–	58.64	20.59	[86]
Ni(15wt %)/ZrO_2	Glycerol (3wt %)	425	252	0.83	–	97	12.92	59.52	[91]
V)	*Catalysts based on yttrium-containing supports*								
Ni(5wt %)/Y_2O_3	Glucose (2wt %)	380	230	–	1	59	26.5	35.85	[56]
Ni(5wt %)/YSZ	Glucose (2wt %)	380	230	–	1	51	11.5	30.35	[56]
Ni(19.5wt %)/$Zr_{0.8}Y_{0.2}O_{2-\delta}$	Glucose (10wt %)	500	230–240	–	0.5	66	22	23.08	[93]
Ni(17.26wt %)/$Zr_{0.4}Ce_{0.4}Y_{0.2}O_{2-\delta}$	Glucose (10wt %)	500	230–240	–	0.5	76	17	42.18	[93]
VI)	*Catalysts supported on ZnO or CaO*								
Ni(5wt %)-Zn(5wt %)/CaO	Empty palm fruit bunches (3.75wt %)	380	–	–	0.5	–	135 mol L^{-1}	2.58	[96]
Ni/ZnO	Glucose (10wt %)	400	241–256	–	0.33	21	0.2	29.41	[83]

 © 2023 The Authors. ChemBioEng Reviews published by Wiley-VCH GmbH

21969744, 0, Downloaded from https://onlinelibrary.wiley.com/doi/10.1002/cben.202300007 by Karlsruher Institution F. Technologie, Wiley Online Library on [26/07/2023]. See the Terms and Conditions (https://onlinelibrary.wiley.com/terms-and-conditions) on Wiley Online Library for rules of use; OA articles are governed by the applicable Creative Commons License

Table 1. Continued.

Catalyst	Feed	Temp. T [°C]	Pressure p [bar]	Space velocity [h^{-1}]	Reaction time [h]	CGE [%]	H_2 yield [mol kg_{feed}^{-1}]	R_{Hb} [%]	Ref.
VII)	*Catalysts supported on TiO_2*								
Ni(10wt %)/TiO_2	Lignin (20wt %)	650	260	–	0.83	–	1.83	–	[65]
Ni(10wt %)-Ce/TiO_2 (Ce/Ni molar ratio = 0.1)	Lignin (20wt %)	650	260	–	0.83	–	1.94	–	[65]
Ni(5wt %)/TiO_2	Glucose (2wt %)	380	230	–	0.25	59	16.7	29.54	[56]
Ni(15wt %)/TiO_2	Glycerol (3wt %)	425	252	0.83	–	95–100	15.96	50	[91]
Ni/TiO_2	Glucose (10wt %)	400	241–256	–	0.33	19.5	2.5	28.57	[83]
Ru(2wt %)/TiO_2	*C. vulgaris* (7.3 wt %)	600	240	–	0.033	65	10	68.45	[14]
Ru(1wt %)/TiO_2	HTL downstream water[b)] (no pure water added)	600	460–520	–	1	88.7	0.91	77.19	[82]
Zn(20wt %)/TiO_2	Furfural 10wt %	400	–	–	0.33	12	17.38	31.36	[98]
Ni(20wt %)/TiO_2	Furfural 10wt %	400	–	–	0.33	10	4.5	51.05	[98]

[a)]SC: synthesis of the catalyst with supercritical water; SG: corresponding sol-gel technique; [b)]HTL: hydrothermal liquefaction of microalgae.

water solution in a batch reactor. Among the catalysts tested, Ni/α-Al_2O_3 had the best performance, as mentioned in Tab. 1. They reported the reasons that make α-Al_2O_3 an ideal support for SCWG of glucose. The first reason is the high reducibility of Ni^{2+} cations on its surface. Secondly, α-Al_2O_3 has high stability under SCW conditions. In contrast, the γ-Al_2O_3 support loses its stability when it is exposed to SCW and undergoes phase transition to boehmite. This transition leads to obstruction of Ni active sites. Furthermore, among all alumina phases, α-alumina has the least acidic sites, which are responsible for tar and higher alkanes formation. Also, α-Al_2O_3 has remarkably high mechanical strength and low solubility in SCW.

Louw et al. [16] compared a Ni/Al_2O_3-SiO_2 catalyst with a homogeneous K_2CO_3 for the SCWG of primary paper waste sludge (PWS). The results shown in Tab. 1 indicate that the heterogeneous Ni catalyst could approach the equilibrium, in contrast to the homogeneous one. The latter catalyst had very high hydrogen yield but half the total gas yield that the Ni catalyst produced, i.e., 18.50 and 40.62 mol kg_{PWS}^{-1}, respectively. The K_2CO_3 catalyst promoted the WGS reaction, while Ni/Al_2O_3-SiO_2 promoted steam reforming and hydrogenations. However, in the study of Okolie et al. [57], where the catalytic SCWG of soybean straw was investigated on different Ni-based catalysts, the Ni/Al_2O_3-SiO_2 had the worst performance in terms of H_2 yield and selectivity. The best two catalysts were Ni/ZrO_2 and Ni/Al_2O_3 reaching H_2 yields of 8.1 and 7 mmol g^{-1}, respectively (Tab. 1), whereas the Ni/Al_2O_3-SiO_2 had only 3.5 mmol g^{-1}. The total gas yield of the Ni/Al_2O_3 was 24.1 mmol g^{-1}, whereas the respective yield of the Ni/ZrO_2 was 17.4 mmol g^{-1}. H_2 selectivity of the Ni/ZrO_2 was double that of the Ni/Al_2O_3. The authors attributed the low H_2 yield of the Ni/Al_2O_3-SiO_2 to the poor dispersion of Ni on the support and to possible hydrogenation reactions. By comparing these two studies, it is obvious that the Ni/Al_2O_3-SiO_2 catalyst from Louw et al. [16] had higher H_2 yield. This difference in performance could be attributed to the significantly higher Ni loading in the catalyst used by Louw et al. [16] (65 wt %) compared to the catalyst used by Okolie et al. [57] (10 wt %).

Kang et al. [58] prepared Ni(2.6wt %)-Co(5.2wt %)/Mg-Al catalysts for hydrogen production via SCWG of lignin. Two different methods for catalyst preparation were tested, namely, the coprecipitation and the impregnation. The catalyst that performed the best was prepared by coprecipitation (Tab. 1). They reported the positive effect of the Ni-based catalyst promoted with Co on hydrogen production and on CH_4 conversion via the steam reforming reaction at relatively high temperature [8, 59]. Cobalt may act as carbon formation inhibitor and this was ascribed to the interaction with the Ni sites in Ni-Co alloys [60].

Li et al. [61] also found that Co acts as a very efficient promoter enhancing hydrogen selectivity for Ni-based catalysts. The beneficial effect of cobalt was confirmed in the study of Sun et al. [62] who reported a 1.44 times increased H_2 yield of a Ni(10wt %)/Al_2O_3 catalyst for hydrothermal gasification of cellulose by adding 6 wt % Co as a promoter (Tab. 1), despite the slightly lower specific surface area of the Co-promoted catalyst. As the loading of Co increased, NiO and Co_3O_4 started to transform into $NiCo_2O_4$, increasing the interaction between Ni and Co and therefore preventing carbon deposition on Ni.

Kang et al. [58] detected also that for the Ni(2.6wt %)-Co(5.2wt %)/Mg-Al catalyst the method of coprecipitation increased the amount of strong acidic sites, when compared to the method of impregnation [59, 63]. Strong acidic sites benefit the lignin decomposition and the accessibility of hydrogen atoms [58, 64]. Kang et al. [60, 61] tested Ce-promoted Ni-based (20 wt % Ni) catalysts supported on Al_2O_3 at SCWG of lignin and cellulose feedstocks. They also tested unpromoted Ni/Al_2O_3 catalysts. The highest gas yield, both from lignin and

 © 2023 The Authors. ChemBioEng Reviews published by Wiley-VCH GmbH

21969744, 0, Downloaded from https://onlinelibrary.wiley.com/doi/10.1002/cben.202300007 by Karlsruher Institution F. Technologie, Wiley Online Library on [26/07/2023]. See the Terms and Conditions (https://onlinelibrary.wiley.com/terms-and-conditions) on Wiley Online Library for rules of use; OA articles are governed by the applicable Creative Commons License

from cellulose, was reported for Ni-Ce/Al_2O_3 (Ce/Ni = 0.36). The Ni-Ce/Al_2O_3 resulted in similar H_2 gas yields from both lignin and cellulose of 2.15 and 1.90 mmol g^{-1}, respectively (Tab. 1).

Ce-promoted catalysts presented higher metal dispersion and better coke resistance. As demonstrated in earlier studies [65, 66], Ce-promotion facilitates Ni dispersion and the weakening of interaction between Ni and Al_2O_3, thus helping its reducibility and the attenuation of carbon formation. Okolie et al. [57] came up with this argument as well, when they used Ce (1 wt %) for the promotion of Ni(10wt %)/Al_2O_3 and Ni(10wt %)/ZrO_2 catalysts for SCWG of soybean straw. In addition, they proposed that Ce promoted steam reforming reactions and the oxidation of carbon deposits.

Promotion of Ni/γ-Al_2O_3 with Cu was also tested recently. Liu et al. [67] used a Ni(10wt %)-Cu/γ-Al_2O_3 for the SCWG of kitchen waste, with different Cu compositions. The highest H_2 yield (727.44 mmol L^{-1}) was attained with 2.5 wt % Cu loading. Apart from promoting the WGS reaction, Cu enlarged the carbon capacity for methane decomposition. However, further addition of Cu suppressed the gasification. Hao et al. [68] performed SCWG of indole and found that the promotion of Ni with Cu on an activated carbon support aided the C–C bond cleavage and the formation of CH_4, provided a large specific surface area to the catalyst, sustained the porous structure of the catalyst during SCWG, and hindered Ni sintering. Other promotions of Ni were Fe, Rb, and Ce, which showed an increase in the CGE and yield of H_2 and CH_4 at SCWG of oilfield sludge [69].

As Li et al. [63] reported, small amounts of Mg in Mg-Al supports could enhance the hydrothermal stability under SCWG due to the formation of $MgAl_2O_4$ and hinder the formation of graphite carbon. However, Mg forms MgO, which retards the reduction of nickel oxides to nickel nanoparticles [63]. In one of their recent studies [59], they tested a Ni (26.3wt %)/$MgAl_2O_4$-Al_2O_3 catalyst prepared by coprecipitation in SCWG of different feedstocks. The catalyst promoted hydrogen production and reached extremely high gasification efficiencies of hydrogen and carbon, i.e., 160 % and 70 %, respectively, with a 5 wt % glucose feed solution (Tab. 1).

A Ni(30wt %)/MgO-Al_2O_3 catalyst and a Ni/Al_2O_3 catalyst, prepared by supercritical water synthesis or SCWS, were used for SCWG of glycerol [70]. Their performances were compared with that of other catalysts that were synthesized by SCWS, including Ni(30wt %)/ZrO_2, Ni(30wt %)/CeO_2-ZrO_2, Ni(30wt %)/activated carbon (AC) and Ni/carbon nanotubes (CNTs). The first two outperformed all the other tested catalysts in terms of CGE and hydrogen yield. Their high H_2, CH_4, and CO_2 yields were attributed to their promotional effect on the reactions of WGS, methanation and of decomposition of organic molecules. It was reported that the Mg promotion led to the formation of the highly dispersed $MgAl_2O_4$ spinel, which enhanced the stability of the Ni/Al_2O_3 pore structure.

Ru-based catalysts supported on Al_2O_3 have been proved effective in SCWG of organic feedstock. Onwudili and Williams [71] performed gasification of glucose, xylan, cellulose, and sawdust in supercritical water using a Ru(5wt %)/α-Al_2O_3 catalyst (Tab. 1). Implementation of this catalyst increased the yield of gaseous products drastically, compared to the noncatalytic gasification. NaOH and CaO addition was proved beneficial by increasing the CH_4 and H_2 yields while decreasing the yield of produced CO_2, since they act as carbon capture agents, producing sodium carbonate and calcium carbonate, respectively. The Ru(5wt %)/α-Al_2O_3 resulted in a CGE of 96 % for glucose SCWG.

Zhang et al. [10] used a RuNi(10wt %)/γ-Al_2O_3 (Ru/Ni molar ratio of 0.1) for the SCWG of glucose as well (Tab. 1). The addition of this catalyst reduced the tar yield effectively. The Ni-Ru/Al_2O_3 bimetallic catalyst was also considered very effective in the SCWG of phenol and especially in catalyzing the reforming of phenol to H_2, the CO methanation, and the WGS reaction [72]. It was shown recently that small Ru nanoparticles, around 1.0 nm, benefit the catalytic performance of glycerol SCWG and that under reaction conditions they tend to form larger particles in the range of 2–3 nm [73].

Promoting a Ru(5wt %)/γ-Al_2O_3 catalyst with Zn for biomass SCWG can increase the total gas yield as well as the H_2 and CO yields. Barati et al. [74] investigated the gasification of bagasse with water under supercritical conditions. The carbon gasification yield and hydrogen production increased significantly with the use of a Ru(5wt %)-Zn(1.5wt %)/γ-Al_2O_3 catalyst (Tab. 1). The promotion with Zn also affected the total gas yield. More specifically, increasing the Zn concentration raised the total gas yield and the H_2 yield, while it decreased the CH_4 yield. They attributed this trend to the blocking effect of Zn on the adsorption of H_2 and CO on the catalyst surface, leading therefore to inhibition of the methanation reaction.

Raney-nickel catalysts have been proved effective in the heterogeneous SCWG process since decades now [13, 75, 76] but they continue to attract research interest. Three different Raney-nickel catalysts were employed by Jin et al. [77] for the SCWG of grounded peanut shell particles at 400 °C, 220–240 bar, and for 20 min reaction time. It was found that they enhance the CGE, two or even three times the value it had without catalyst. The highest CGE was obtained with the Raney-nickel catalyst which contained ~90 wt % Ni and was promoted with 1 wt % Mo. While the one promoted with such a low Mo loading provided the highest CGE, the one that resulted in the highest H_2 yield was the one promoted with 15 wt % Fe.

Chen et al. [78] tested also Raney-Ni(93.57wt %) catalysts promoted with Mo (0.34 and 0.31 wt %) and Fe (7.86 wt %) for the SCWG of sewage sludge (Tab. 1). They found that both the highest CGE and the highest H_2 selectivity were achieved with the Raney-nickel catalysts with 0.31 wt % Mo. This catalyst exhibited higher catalytic activity because of its larger specific surface area and pore volume. Their experiments were conducted under low temperatures (350–450 °C), hence the methanation and the WGS could be promoted, especially when the catalyst loading was increased from 0.2 to 1.4 $g_{catalyst}$ g_{sludge}^{-1}. They reported that the raise in catalyst loading increased the CGE and the total gas yield but it decreased slightly the H_2 selectivity.

Sheikhdavoodi et al. [11] studied the SCWG of sugarcane bagasse on a commercial Raney-nickel catalyst with 50 wt % solid catalyst and reached approximately similar CO_2 and CH_4 yields that were very high in comparison with the H_2 yield (Tab. 1). They argued that Raney-nickel facilitates the C–C

 © 2023 The Authors. ChemBioEng Reviews published by Wiley-VCH GmbH

21969744, 0, Downloaded from https://onlinelibrary.wiley.com/doi/10.1002/cben.202300007 by Karlsruher Institution F. Technologie, Wiley Online Library on [26/07/2023]. See the Terms and Conditions (https://onlinelibrary.wiley.com/terms-and-conditions) on Wiley Online Library for rules of use; OA articles are governed by the applicable Creative Commons License

bond cleavage and that it is a very efficient catalyst in CO hydrogenation/methanation. Its CGE, however, was only 53.1 % and this was attributed to the increased amount of sulfur in bagasse. Their results regarding hydrogen production were comparable with the ones by Azadi et al. [15] who showed that the H_2 selectivity from the SCWG of different biomass resources on a Raney-Ni catalyst (50 wt % solid content) was lower from the corresponding values on a Ni(5wt %)/Al_2O_3 or a Ni(5wt %)/hydrotalcite. In their study, however, Raney-nickel demonstrated the highest CGE.

Tiong et al. [75] examined the SCWG of two different microalgae species on a Ni(12wt %)/α-Al_2O_3 and a Raney-Ni(68.2wt %) catalyst in a batch reactor at 385 °C, 260 bar for short and long reaction times, i.e., 15 and 90 min, respectively. Regardless of the feed, the Raney-nickel catalyst showed higher CGE and higher H_2 and CH_4 yields than the Ni/α-Al_2O_3. The Raney-nickel catalyst contained traces of Na, which possibly enhances hydrogen production. The substantial difference in the activity of the two catalysts could be ascribed to the different surface areas, with the Raney-nickel having a larger surface area than the Ni/α-Al_2O_3.

Alumina can be considered as the most common support for metal oxide catalysts, in the forms of α-Al_2O_3 and γ-Al_2O_3. Many researchers prefer α-Al_2O_3 due to its overall better performance under supercritical water. Both Ni and Ru are commonly used as active metals on Al_2O_3. The effect of the active metal promoters on the catalytic performance has been widely studied on this support with the more efficient ones being Ru, Mo, and Co. Promoters of the Al_2O_3 support are also investigated. According to the literature data, coprecipitation and the SCWS methods are considered the most effective.

2.2 Catalysts Based on CeO_2

Ceria, well-known for its redox behavior, has been also used as support in SCWG. Lu et al. [66] conducted SCWG of glucose utilizing Ni catalysts with different supports in order to compare their performances, as reported in Tab. 1. Based on hydrogen yield, they ended up in the following descending order: CeO_2-Al_2O_3 > La_2O_3-Al_2O_3 > MgO-Al_2O_3 > Al_2O_3 > ZrO_2-Al_2O_3. The descending order, based on H_2 selectivity was: CeO_2-Al_2O_3 > La_2O_3-Al_2O_3 > ZrO_2-Al_2O_3 > Al_2O_3 > MgO-Al_2O_3. Regarding the carbon formation, they observed that graphitic coke was formed on Ni catalysts supported on mixed La-Al, Zr-Al, and Mg-Al oxides; amorphous carbon, on the other hand, was formed on alumina. No significant carbon formation was observed on Ni supported on mixed Ce-Al. They argued that the redox properties of ceria and its high oxygen storage capacity and mobility played a significant role in the prevention of carbon formation.

Lu et al. [79] also demonstrated the superiority of a Ni(20wt %)/CeO_2-γ-Al_2O_3 over a Ni(20wt %)/γ-Al_2O_3 catalyst for the gasification of glucose under supercritical water conditions. The results are given in Tab. 1. The performance superiority was firstly based on the higher H_2 yield and selectivity and, secondly, on the better resistance to coke deposition. However, the surfaces of the used catalysts were covered with carbon and agglomeration of the Ni particles was also apparent. Nevertheless, the carbon formed on Ni/γ-Al_2O_3 was of graphitic structure, whereas that on the Ni/$CeO_{2\text{-}\gamma}$-Al_2O_3 was of filamentous type. In another study, addition of CeO_2 on Al_2O_3 support was found to suppress the formation of carbon filaments on a Ni catalyst [80]. In addition, the effect of Ce loading in a Ni(20wt %)/CeO_2-Al_2O_3 on the H_2 yield and on its selectivity [81] was explored, with the maximum H_2 yield attained for CeO_2 loading of 8.46 wt % out of a range of 1.22–10.83 wt %.

In another study [82], which dealt with SCWG of the downstream water from microalgae hydrothermal liquefaction, a Ru(1wt %)/CeO_2 catalyst was used and its H_2 and CH_4 yields were the highest among all the other Ru-based catalysts. However, it did not have the highest CGE.

In most of the studies, ceria was selected as a support in mixture with Al_2O_3 for Ni-based catalysts. It is therefore considered that the ability of ceria to prevent carbon formation was combined with the ability of alumina to provide supports of large surface area and high mechanical and thermal stability as well.

2.3 Catalysts Based on MgO

Ding et al. [80] reported that a Ni(10wt %)/MgO catalyst increases the H_2 yield of glucose SCWG process by 62 % (Tab. 1), compared to the noncatalytic process and other Ni-based catalysts, a Ni(10wt %)/Al_2O_3 and a Ni(10wt %)/CeO_2/Al_2O_3. Yin et al. [83] described similar results for maximum H_2 yield with a Ni/MgO catalyst, among other heterogeneous catalysts. Apart from the H_2 yield, the CGE was also the highest for the Ni/MgO. However, similar CH_4 composition among all the tested Ni-based catalysts was reported indicating that Ni/MgO catalysts promote effectively the WGS reaction.

Mastuli et al. [84] synthesized Ni-Mg solid solutions as catalysts for SCWG of oil palm leaves. They reported an increase in H_2 and CO_2 concentration in the product gas with increasing Ni content. This behavior was related to the WGS reaction that was promoted by the Ni catalyst and to the unpromoted methanation reaction. $Mg_{0.8}Ni_{0.2}O$ exhibited the highest number of basic sites that react with H_2O, producing H_2. The results from its activity are given in Tab. 1. It also had the largest surface area and the smallest crystallite size. The authors tested later the doped $Mg_{0.95}Ni_{0.05}O$ catalyst with a Ni-based one supported on MgO (Ni/MgO) [85]. They found that the supported Ni/MgO catalyst generated lower H_2 and higher CO composition than the MgO with a dopant of 5 wt % Ni. They ascribed this to the higher dispersion of the active metal and the specific surface area of the doped catalyst than that of the supported catalyst.

Liu et al. [86] demonstrated that the promotion of Ni(20wt %)/ZrO_2 with MgO increases the H_2 yield in SCWG of glycerol (Tab. 1). They argued that the promotion with MgO leads to the formation of alkaline centers on the catalyst surface, which adsorb acidic intermediates. The alkaline centers of the MgO support act mainly as catalytic sites for the decomposition and generation of intermediate reactive compounds forming light gas products [87]. A drawback is that they can form char-like carbonaceous species and also form $Mg(OH)_2$, which has lower catalytic activity [88].

 © 2023 The Authors. ChemBioEng Reviews published by Wiley-VCH GmbH

21969744, 0, Downloaded from https://onlinelibrary.wiley.com/doi/10.1002/cben.202300007 by Karlsruher Institution F. Technologie, Wiley Online Library on [26/07/2023]. See the Terms and Conditions (https://onlinelibrary.wiley.com/terms-and-conditions) on Wiley Online Library for rules of use; OA articles are governed by the applicable Creative Commons License

2.4 Catalysts Based on ZrO_2

Okolie et al. [57] prepared a Ni(10wt %)/ZrO_2 with superior H_2 yield against all other catalysts, that were Ni-based (with 10 wt % Ni) as well, but on different supports, namely, Al_2O_3, Al_2O_3-SiO_2, activated carbon, SiO_2, and CNTs. The main reasons for this were ascribed to the high Ni dispersion on ZrO_2 support, strong metal-support interaction, minimized coke formation, and the ability of the catalyst to participate in reactions between intermediate products and reactants.

In a study where SCWG of a model polyethylene glycol wastewater was carried out [89], different active metals all supported on ZrO_2, namely, Ni(15wt %)/ZrO_2, Co(15wt %)/ZrO_2, W(15wt %)/ZrO_2, Ni(15wt %)-Co(5wt%)/ZrO_2, and Ni(15wt %)-W(5wt %)/ZrO_2, were tested for their performance in terms of gas product yields, gasification, and H_2 efficiencies. The study revealed the crucial role of ZrO_2, inhibiting the methanation and providing a 2.7 times higher H_2 yield than the noncatalytic case. Among the various metals used, the activity of Ni was higher than that of Co and W (Tab. 1). Zhu et al. [90] and Liu et al. [86] attributed this to the ability of this catalyst to promote the WGS reaction.

Zhu et al. [90] tested different compositions of Ni/ZrO_2 for the SCWG of glycerol. The catalyst with the highest activity in their study was the Ni/ZrO_2 with a molar ratio of Ni^{2+}/Zr^{4+} = 0.4:0.6. This catalyst, compared to the SCWG without a heterogeneous catalyst, reached approximately double H_2 and CO_2 yields and the smallest CO yield. Liu et al. [86] tested also Ni/ZrO_2 catalysts with varying Ni loading from 5 wt % up to 20 wt % for glycerol SCWG. From their results it could be concluded that the highest H_2 yield was attained with the highest Ni loading catalyst. Similarly with the above researchers, Li et al. [91] prepared a Ni(15wt %)/ZrO_2 catalyst, which performed stably in the SCWG of glycerol under 80 h time-on-stream (TOS). The presence of the catalyst was beneficial as a 3-fold, 5-fold, and a 150-fold increase in H_2, CO_2, and CH_4 yields, respectively, were observed, compared with the same noncatalytic experiments. The CGE of the catalyst was approx. 97 %. It was reported that the phase and pore structure of Ni/ZrO_2 were altered during exposure under the SCWG conditions for this long TOS, a process called catalyst in-situ activation.

Another factor found to strongly affect the structure of the Ni/ZrO_2 catalyst and therefore its activity is the calcination temperature [92]. Kou et al. [92] performed SCWG of a diesel solution in an autoclave at 500 °C, 235–245 bar, and for 30 min reaction time. They used Ni/ZrO_2 catalysts with different calcination temperatures and found that low calcination temperatures in the range of 500–600 °C led to Ni crystallites with sizes similar to that of the support pores, which were around 20 nm. Thus, the Ni particles blocked the pores of the support, totally prohibiting the diffusion of the reactants. High calcination temperatures (800 °C), on the other hand, led to microporous or nonporous structures upon which the Ni particles formed agglomerates. Medium calcination temperatures of 650 °C up to 750 °C provided catalysts with wide pore distributions. The highest carbon gasification efficiency was achieved in the presence of the catalyst with a calcination temperature of 700 °C. This catalyst had a Ni loading of 17.9 wt % while the loading of the other catalysts ranged from 17.3 to 17.5 wt %.

Zirconia is a highly promising support for Ni-based catalysts. It interacts strongly with Ni and thus prevents its sintering and coke formation. It provides also high dispersion to the active metal.

2.5 Catalysts Based on Oxides that Contain Yttrium (Y)

As reported previously in Sect. 2.1, Azadi et al. [56] tested also Ni-based catalysts with 5 wt % loading supported on two yttrium-containing supports, Y_2O_3 and YSZ, short for yttria stabilized zirconia, for the SCWG of glucose. They observed that the Ni/Y_2O_3 catalyst resulted in a moderate CGE and in a high hydrogen gasification efficiency (Tab. 1). This catalyst generated H_2 with a yield among the highest found in this study. Ni/YSZ did not perform as well as Ni/Y_2O_3. In comparison with other catalysts, Ni/Y_2O_3 was the third most active catalyst in terms of H_2 yield and selectivity, after Ni/CNTs and Ni/MgO. Ni/YSZ surpassed Ni/CeO_2, Ni/AC, and Ni/ZrO_2. YSZ was found to be the only stable catalyst support after 1 h of exposure at SCW, without any structural alterations.

Another team of researchers employed a Ni/$Zr_{0.8}Y_{0.2}O_{2-\delta}$ catalyst with varying Ni content for the gasification of glucose with supercritical water [93]. The maximum hydrogen yield and selectivity were reported for the $Ni_{0.5}/Zr_{0.8}Y_{0.2}O_{2-\delta}$ (Tab. 1), which was ten times the yield without catalyst. The very low concentration of CO indicated that the catalyst effectively promoted the WGS reaction and the hydrogenation of CO as well. Addition of CeO_2 to the support to enhance the gasification efficiency did not have any positive effect. Compared with the activity of the $Ni_{0.5}/Zr_{0.8}Y_{0.2}O_{2-\delta}$ catalyst, the $Ni_{0.5}/Zr_{0.4}Ce_{0.4}Y_{0.2}O_{2-\delta}$ decreased the H_2 yield and selectivity, whereas it increased the CH_4 yield. It was therefore argued that CeO_2 addition promoted further the methanation reaction.

Yttrium was also employed as promoter of Ni(25wt %)/activated carbon for the SCWG of valine [94], where it showed high activity in reforming light hydrocarbons such as C_2H_6 and C_3H_8 and in the WGS reaction.

Three different types of Y-containing support for Ni-based catalysts for the SCWG of glucose were found in the literature, the Y_2O_3, the YSZ and the Ce-promoted YSZ. It was found that all catalysts gasify efficiently glucose and promote methanation, but the higher CGE and CH_4 yield were obtained with the Ni-based catalyst supported on YSZ promoted with Ce.

2.6 Catalysts Based on ZnO

Sinağ et al. [95] used ZnO and SnO_2 as active catalytic components for the gasification of cellulose at different reaction temperatures. The ZnO formed mostly H_2 and CO_2 at low temperatures, i.e., 300 °C and subcritical pressure, i.e., 80 bar, while the SnO_2 generated also a considerable amount of CO, indicating that only the ZnO catalyzes effectively the WGS reaction. At higher temperatures, they reported the increase in the content

21969744, 0, Downloaded from https://onlinelibrary.wiley.com/doi/10.1002/cben.202300007 by Karlsruher Institution F. Technologie, Wiley Online Library on [26/07/2023]. See the Terms and Conditions (https://onlinelibrary.wiley.com/terms-and-conditions) on Wiley Online Library for rules of use; OA articles are governed by the applicable Creative Commons License

of hydrocarbons, attributed mainly to the catalytic effect of the autoclave wall. The utilization of ZnO for sulfur removal upstream of catalytic beds in continuous microalgae SCWG processes kept the catalyst active for 55 h of operation, under 400 °C and 280–290 bar [28, 46].

Yin et al. [83] tested a Ni/ZnO catalyst in glucose SCWG (Tab. 1). It was shown that Ni/ZnO could multiply the H_2 gas yield observed at noncatalytic gasification by approximately five times. Its carbon gasification efficiency was the second highest after that of Ni/MgO. However, Ni/ZnO generated the lowest volume percentage of H_2 compared with the other tested catalysts in this study: Ni/MgO, Ni/Al_2O_3, and Ni/TiO_2, while its CO and CO_2 concentrations were the highest.

Sivasangar et al. [96] used ZnO (5 wt % Zn) as a catalytic dopant into Ni(5wt %)/CaO, resulting in the highest H_2 yield (Tab. 1) among other tested Ni(5wt %)/CaO catalysts, which were doped with other elements. It was mentioned in this study that the catalyst doped with ZnO consisted of metallic Ni, ZnO, and Ni_8Zn_2O supported on CaO. The latter structure was highly effective in the WGS reaction, the steam reforming reactions, and the cleavage of C–C bonds, as the researchers stated. They also observed an enhancement of the methanation reaction with longer reaction time.

Cao et al. [97] tested different molar ratios of CuO/ZnO for lignin SCWG. A higher content of CuO resulted in higher CGE but lower H_2 selectivity. They attributed these findings to the weaker bond of Cu–O than the Zn–O bond that meant higher reduction rate of the CuO species and thus, more active oxygen species. The larger amount of active oxygen promoted the decomposition of lignin but at the same time promoted the oxidization of H_2 and carbon formed on the catalyst. Their best performing catalyst was CuO(50wt %)/ZnO(50wt %) and its activity is given in Tab. 1.

Integrating ZnO as a dopant of the active metal, mostly nickel, is an approach that has been proven beneficial for the generation of hydrogen from the SCWG of organic compounds. Zinc is known for its promotion of the WGS reaction. However, the utilization of zinc oxide as a support for Ni proved to be less efficient than other oxides in terms of H_2 yield and CGE.

2.7 Catalysts Supported on TiO_2

In the study of Azadi et al. [56], the Ni(5wt %)/TiO_2, demonstrated moderate CGE of 60 % and high H_2 yield of around 16 mol kg^{-1}, in the SCWG of glucose (Tab. 1). The yields of CO and CH_4 were in the range of 0.3–0.6 mol kg^{-1} and 1.8 – 3.5 mol kg^{-1}, respectively. The range of CO_2 yields were comparable with that of H_2. At higher concentration of glucose (10 wt % solution), it was shown elsewhere [83] that the CGE and the H_2 yield of a Ni/TiO_2 were reduced significantly, but no information about the active metal loading could be found. Kang et al. [65] demonstrated the better activity of a Ni(10wt %)/TiO_2 against other Ni-based catalysts with different supports, e.g., MgO and ZrO_2. The addition of Ce (Ce/Ni molar ratio of 0.1) slightly enhanced the H_2 yield and decreased the CGE. The improvement in H_2 yield was attributed to the increased Ni dispersion.

Another team compared catalysts on TiO_2 support but with different active metals (Ni, Zn, Cu, and Co) [98]. They found that the Ni-based catalyst performed better in terms of stability under SCWG conditions for 20 min of reaction time, whereas the Zn-based catalyst had the highest H_2 yield. Li et al. [91] prepared Ni-based catalysts (15 wt % Ni) supported on TiO_2, ZrO_2, and Ta_2O_5. They evaluated these catalysts in a continuous SCWG process of glycerol. It was found that while the Ni/TiO_2 catalyst gasified the glucose very effectively, its activity gradually decreased with TOS. From their analysis of the morphology of the used catalysts, it turned out that the Ni particles in the Ni/TiO_2 had formed aggregates and $NiTiO_3$. They also reported the formation of a superficial layer of deactivating graphite. Tab. 1 demonstrates these results.

Chakinala et al. [14] used a Ru(2wt %)/TiO_2 catalyst in the gasification of microalgae in supercritical water and compared their results with a noncatalytic experiment under similar conditions. The Ru/TiO_2 catalyst reached complete gasification of algae at 700 °C. In the SCWG of downstream water from hydrothermal liquefaction from Shan et al. [82], Ru(1wt %)/TiO_2 had a higher CGE than all the other Ru-based catalysts supported on other metal oxides: CeO_2, ZrO_2, Al_2O_3, MgO.

Titania is an effective support for Ni- and Ru-based catalysts, which showed high gasification efficiencies and satisfying CH_4 and H_2 yields. The Ru-based catalysts performed better than the Ni-based ones in terms of CGE and CH_4 yield, even with more complex biomass resources.

From Tab. 1 it can be concluded that the best performing catalysts in terms of high CGE and high H_2 yield, i.e., low R_{Hb} (ratio of hydrogen bound in hydrocarbons to total produced hydrogen) were a Ru-Ni(10wt %)/γ-Al_2O_3 with a Ru/Ni molar ratio of 0.1 and a Ni(20wt %)/MgO-ZrO_2. These two catalysts were highly efficient in gasifying dilute feedstocks of biomass model compounds. They likely promote the reactions of SMR and WGS in the gas phase resulting in high H_2 yield of around 54 mol kg_{feed}^{-1} for the Ru-Ni/γ-Al_2O_3 and 71 mol kg_{feed}^{-1} for the Ni/MgO-ZrO_2 and consequently in low R_{Hb} ratios. The main characteristic of the SCWG operating conditions under which these catalysts were evaluated, were temperatures in the range of 700–800 °C and pressures between 240 and 245 bar. This is indicative of the harsh conditions in terms of temperature needed during gasification with supercritical water to achieve high H_2 production. It should be stressed though that the feeds used were model compounds highly diluted in water and not real residual biomass.

On the other hand, catalysts tested under lower temperatures, i.e., 400–600 °C and medium to high pressures, i.e., 250–500 bar, were efficient in attaining CGEs over 50 % and very high R_{Hb} ratio in the range of 60–99 %, which means that a high percentage of hydrogen was bound in the light hydrocarbons formed. In these cases, Ru as active metal or the Raney-Ni or the Ni(15wt %)/ZrO_2 proved to be very active catalysts. More specifically, Ru on α-Al_2O_3 or TiO_2 or CeO_2, with low concentrations in the range 1–5 wt %, achieved CGEs in the range of 83–96 % and R_{Hb} 63–77.6 % for dilute feedstocks of cellulose and glucose, but also for actual feedstocks such as the downstream water from an hydrothermal liquefaction (HTL) process. The same trend was observed for the two other catalysts, Raney-Ni and Ni(15wt %)/ZrO_2, which

These are not the final page numbers! ↗↗

21969744, 0, Downloaded from https://onlinelibrary.wiley.com/doi/10.1002/cben.202300007 by Karlsruher Institution F. Technologie, Wiley Online Library on [26/07/2023]. See the Terms and Conditions (https://onlinelibrary.wiley.com/terms-and-conditions) on Wiley Online Library for rules of use; OA articles are governed by the applicable Creative Commons License

were subjected to low temperatures (385 °C and 425 °C) and medium pressures (260 and 252 bar), respectively. In particular, the Raney-Ni yielded a very high R_{Hb} ratio of 95 %, with a dilute feed of 5 wt % *Chlorella vulgaris*.

Overall, the presence of catalysts in SCWG is highly beneficial for the carbon gasification efficiency under mild conditions and in most of the cases the R_{Hb} ratio achieved is greater than 30 %, i.e., a significant amount of the produced hydrogen is bound in the form of H–C bonds in the produced hydrocarbons, mostly in methane.

3 Catalysts for Hydrocarbons Reforming

The literature gathered in the previous chapter leads to the conclusion that most of the catalysts were efficient in gasifying bio-based feedstocks generating enough hydrogen, part of which was bound with carbon in light hydrocarbon molecules. In order to obtain the highest possible amount of hydrogen in the form of $H_{2(g)}$, a downstream process is needed that will upgrade the SCWG product gas. This process should be catalytic aiming at the highest possible conversion of the hydrocarbons into H_2, CO, and CO_2. This is done by implementing catalysts that are active either in steam and/or dry reforming of hydrocarbons.

Therefore, this chapter focuses on metal-based catalysts for the steam and dry reforming of the intermediates of SCWG, namely, methane and higher hydrocarbons, covering the research progress that has been performed over the last decade. With this approach an integrated overview of the catalysts and the processes for maximizing the hydrogen formed from residual biomass is provided covering the gap in the open literature.

Catalysts are divided into categories, depending on their support, as in Sect. 2. The parameters used for the evaluation of the catalytic activity and performance are the yields of the desired products, i.e., H_2 and CO, the conversion rates of CH_4 and other hydrocarbons as well:

$$Y_{H_2} = \frac{n_{H_2(\text{produced})}}{RR_{H_2} \times n_{C_nH_m(\text{in})}} \tag{16}$$

$$Y_{CO} = \frac{n_{CO(\text{produced})}}{RR_{CO} \times n_{C_nH_m(\text{in})}} \tag{17}$$

$$\text{Hydrocarbons conversion} = \frac{n_{C_nH_m(\text{in})} - n_{C_nH_m(\text{out})}}{n_{C_nH_m(\text{in})}} \tag{18}$$

In Eq. (16) and Eq. (17) the RR_{H_2} and RR_{CO} are the stoichiometric factors from the reforming reactions of the hydrocarbon C_nH_m. For example, for the SMR reaction, RR_{H_2} = 3 and RR_{CO} = 1, respectively. In many studies, the selectivity of CO and H_2 are also used. These two parameters refer to the ability of the catalyst to drive the products distribution in favor of the desired product and can be given as follows:

$$H_2 \text{ selectivity}(\%) = \frac{n_{H_2(\text{out})}}{n_{CH_4(\text{in})} - n_{CH_4(\text{out})}} \times 100 \tag{19}$$

$$\text{CO selectivity}(\%) = \frac{n_{CO(\text{out})}}{n_{CH_4(\text{in})} - n_{CH_4(\text{out})}} \times 100 \tag{20}$$

3.1 Al_2O_3-Supported Catalysts

Karakaya et al. [99] tested different catalysts based on Rh, Pt, Ru, and Ni supported on alumina, for syngas production via SMR. Rh(2wt %)/δ-Al_2O_3 was the most active catalyst in terms of CH_4 conversion and CO selectivity. The Ni-based catalyst (10wt % Ni) came second in terms of CH_4 conversion. The activity of the first catalyst remained quite stable, i.e., methane conversion was between 65–75 % and CO selectivity around 20 %. The activity of Ni(10wt %)/δ-Al_2O_3 corresponded to methane conversion between 30–40 % and CO selectivity between 10–20 %. Rh was the most CO-selective among the catalysts and next was Pt. Ru and Ni had similar CO selectivity. The data from these catalysts can be found in Tab. 2.

Further studies regarding Rh as active metal in steam reforming and with alumina as its support have been conducted [100, 101]. Zapf et al. [101] synthesized nanoparticles of Rh via the chemical reduction method and used them as precursor for the Rh/Al_2O_3 catalysts for propane steam reforming. By reducing the Rh content from 5 to 2.5 and 1 wt %, the catalysts remained active enough.

Malaibari et al. [102] used a catalyst with 15 wt % Ni/Al_2O_3 with amounts of Mo 0.1 and 0.5 wt % for oxidative and simple steam reforming of propane. Experiments under steam reforming showed that the 0.1 wt % Mo sustained the highest propane conversion during 6 h TOS (Tab. 2). The catalyst promoted with 0.5 wt % Mo had the lowest conversion but the H_2 and CO yield were higher for 0.5 wt % Mo. The CO_2 yield was almost similar for the 0.1 wt % promoted catalyst and the unpromoted and much lower for the 0.5 wt % Mo catalyst. By measuring also the catalytic bed weights after the experiments, the authors reported that the unpromoted catalyst had a weight gain of 30 % via the formation of carbon, whereas the catalyst promoted with 0.1 wt % Mo had a weight gain by 6 %. This indicated that Mo improved the resistance to carbon formation and deposition. They observed also that by the addition of Mo, NiO reduction temperatures were shifted to lower values and more Ni was present as NiO rather than $NiAl_2O_4$. Low Mo loading however, did not have any effect on Ni dispersion.

In general, Mo and other non-noble metals, such as Cu, Sn, Re, and W, have been found to act as inhibitors of coke formation, enhancing the interaction of Ni with the support and altering the Ni^{2+} redox properties [103, 104]. As far as Mo is regarded, species of MoO_x at the catalyst surface interact with Ni by transferring their electrons to it, increasing its electron density and therefore preventing carbon formation [105]. However, Mo addition may not result always in enhanced catalytic activity [106]. Yao et al. [106] investigated a bimetallic Ni(10wt %)-Mo(10wt %)/Al_2O_3 catalyst, a Ni(10wt %)/Al_2O_3 catalyst, and a Mo(10wt %)/Al_2O_3 catalyst for DRM, under 550–850 °C and atmospheric pressure. From their results it was apparent that the Ni-Mo/Al_2O_3 catalyst had lower CH_4 and CO_2 conversion than the unpromoted Ni-based catalyst. The reduced performance of the bimetallic catalyst was attributed to three main reasons. First reason was the lack and/or weakness of basic sites, i.e., lower basicity, which promote the DRM activity. Secondly, $MoNi_4$ species formed that inhibit Ni dispersion since Ni is not any longer widely present as a separate Ni^0 phase. Ni^0 are the sites that are responsible for methane

21969744, 0, Downloaded from https://onlinelibrary.wiley.com/doi/10.1002/cben.202300007 by Karlsruher Institution F. Technologie, Wiley Online Library on [26/07/2023]. See the Terms and Conditions (https://onlinelibrary.wiley.com/terms-and-conditions) on Wiley Online Library for rules of use; OA articles are governed by the applicable Creative Commons License

Table 2. Catalysts for hydrocarbons reforming based on Al_2O_3 supports and their performance in terms of hydrocarbons conversion and H_2 yield, not only initially but also after TOS. The conditions to which each catalyst was subjected are also recorded, i.e. temperature, feed and space velocity. The pressure was in all cases atmospheric unless otherwise specified.

Type	Temp. [°C]	Feed ratio	TOS [h]	Space velocity or residence time	Hydrocarbons conversion [%]		H_2 yield		Ref.
					Initial	After TOS	Initial	After TOS	
Rh(2wt %)/δ-Al_2O_3	800	S/CH_4 (3:1)	72	155.4 L g_{cat}^{-1} h^{-1}	75	65–75	–	–	[99]
Ni(10wt %)/δ-Al_2O_3	800	S/CH_4 (3:1)	72	147.6 L g_{cat}^{-1} h^{-1}	40	30–40	–	–	[99]
Rh(5wt %)/Al_2O_3	750	S/C_3H_8 (4:1)	120	120 L g_{cat}^{-1} h^{-1}	100	100	–	–	[101]
Ni(15wt %)-Mo(0.1wt %)/γ-Al_2O_3	450	S/C_3H_8 (3:1)	6	339.8 L g_{cat}^{-1} h^{-1}	76	76	6 mol mol_{C3H8}^{-1}	6 mol mol_{C3H8}^{-1}	[102]
Ni(15wt %)-Mo(0.5wt %)/γ-Al_2O_3	450	S/C_3H_8 (3:1)	6	339.8 L g_{cat}^{-1} h^{-1}	50	50	8 mol mol_{C3H8}^{-1}	8 mol mol_{C3H8}^{-1}	[102]
$SrNiO_3$/γ-Al_2O_3	700	CO_2/C_3H_8 (3:1)	50	6 L g_{cat}^{-1} h^{-1}	88	88	–	–	[103]
Ni(10wt %)- Re/$Ce_{0.5}Zr_{0.5}O_2$/Al_2O_3 Re/Ni=0.03	850	S/CH_4/O_2 (1:1:0.75)	25	24 L g_{cat}^{-1} h^{-1}	100	–	67%	67%	[104]
Ni(10wt %)-Mo(10wt %)/Al_2O_3	850	CH_4/CO_2 (1:1)	–	20,000 h^{-1}	90	–	–	–	[106]
Ni(15wt %)-Ag(0.3wt %)/Al_2O_3	600	S/CH_4 (1:2)	6	105 L g_{cat}^{-1} h^{-1}	20	20	–	–	[107]
Ru(3.1wt %)/γ-Al_2O_3	700	S/Biogas (3:2), CH_4/CO_2 (3:2)	0.5	850 h^{-1}	95	95	60%	60%	[119]
Ni(7.4wt %)/$NiAl_2O_4$/γ-Al_2O_3	850		0.5	850 h^{-1}	100	100	60%	60%	[119]
Ni(20wt %)/γ-Al_2O_3	900	S/CH_4 (3:1)	12	240,000 h^{-1}	86[a)]	85	–	–	[120]
Ni(20wt %)/Al_2O_3 (SG)[b)]	500	S/C_3H_8 (4:1)	19	204 L g_{cat}^{-1} h^{-1}	65	55	50%	45%	[121]
Ni-Co/Al_2O_3, Ni/Co mass ratio = 2:1, total active metals load = 20wt %	700	S/CH_4 (2:1)	12	37 L g_{cat}^{-1} h^{-1}	91	88.4	86	82	[115]
Ni(10wt %)-Co(10wt %)-Ce(1wt %)/Al_2O_3	700	S/CH_4 (2:1)	12	37 L g_{cat}^{-1} h^{-1}	97.3	92	99	94	[113]
Pt(1wt %)/$Ce_{0.8}Nb_{0.2}O_2$ (20wt %)/Al_2O_3	800	S/CH_4 (3:1)	400	80,000 h^{-1}	95	50	–	–	[110]
Ni(10wt %)/Nb(10wt %)-Al_2O_3	550	S/CH_4 (2:1)	24	28.8 L g_{cat}^{-1} h^{-1}	45	40	–	–	[111]
Ni(20wt %)-Ce(3wt %)/Al_2O_3	700	S/C	12	30 L g_{cat}^{-1} h^{-1}	88	84.03	97.5	92.4	[116]
Ni(20wt %)-Ce(1.5wt %)/Al_2O_3	700	S/CH_4 (2:1)	12	37 L g_{cat}^{-1} h^{-1}	90	86	98	85.5	[117]

[a)]Pressure: 20 bar; [b)]SG: sol-gel technique for the preparation of the catalyst.

 © 2023 The Authors. ChemBioEng Reviews published by Wiley-VCH GmbH

21969744, 0, Downloaded from https://onlinelibrary.wiley.com/doi/10.1002/cben.202300007 by Karlsruher Institution F. Technologie, Wiley Online Library on [26/07/2023]. See the Terms and Conditions (https://onlinelibrary.wiley.com/terms-and-conditions) on Wiley Online Library for rules of use; OA articles are governed by the applicable Creative Commons License

decomposition. The third reason was the weak interaction between NiO and Al_2O_3. More information about these catalysts regarding their activity can be found in Tab. 2.

The effect of adding other metals in Ni/Al_2O_3 such as Ag has also been investigated [107–109]. Ag can change the superficial structure of Ni sites and decrease the carbon deposition rate on Ni [107]. A team of researchers [108, 109] examined the mechanism and the effect of Ni sites substitution with Ag on the catalyst performance and stability. They found that an increase in Ag fraction on the surface of the Ni catalyst leads to an increment in the energy required for activation of the C–H bond in the CH_4 molecule, which is the basic reaction step in steam reforming on Ni-based catalysts [108]. The substitution of Ni with Ag affects in a negative manner the Ni dispersion as well [108]. They argued that Ag serves not only as a blocking agent of the more active Ni sites, but also as a modifying agent of the adjacent Ni sites around substitute Ag atoms on the catalyst, making them inactive to C–H activation [108]. This fact has a negative effect on the turnover frequency on these catalysts. Ag can, at the same time, block the carbon nucleation sites and it can prevent the formation of filamentous carbon as well [109].

Matus et al. [104] conducted a study, which compared different bimetallic catalysts in the autothermal reforming of methane, also known as ATR. The catalysts had the chemical formula Ni(10wt %)-M/ $Ce_{0.5}Zr_{0.5}O_2/Al_2O_3$ with M being Pt, Pd, Re, Mo or Sn and with a molar ratio M/Ni = 0.003, 0.01 or 0.03. For temperatures of 850–900 °C, bimetallic catalysts with Pt, Pd, Re, and Mo provided CH_4 conversions of at least 50 % and even almost 100 %. However, almost complete CH_4 conversion at the lower applied temperature range was given by the two bimetallic catalysts that contained noble metals, the Ni-Pt and Ni-Pd. Pt has been used lately as active metal in Pt(1wt %)/ $Ce_{0.8}Me_{0.2}O_2/Al_2O_3$ (with Me being Gd, Nb, Pr and Zr) catalysts for SMR at 800 °C, different gas hourly space velocities (GHSVs) and at 400 h TOS [110]. The primary cause of deactivation seemed to be the sintering of active metal and the most active and stable catalyst was the one with Nb in its support (Tab. 2). Niobium was believed to stabilize the alumina by forming $AlNbO_4$ and to aid in the stronger interaction between Pt and Nb_2O_5. Zeng et al. [111] tested a 10 wt % Ni-based catalyst supported on Nb(10wt %)-Al_2O_3 for SMR (Tab. 2). Prior to experiments, they tried three different treatments, the first with H_2, the second with N_2, and the last with air, all at 600 °C for 2 h. The treatment with H_2 increased the Ni-Nb interaction and formed small homogeneous Ni particles (6 nm) that were stable during the reaction.

The use of Co as promoter of Ni has been considered beneficial. Its use in Ni-based catalysts in SMR can promote carbon gasification due to its high oxygen mobility [112, 113]. Another positive aspect is the formation of Ni-Co alloys, which hinder carbon formation [114, 115]. Zarei-Jelyani et al. [115] tried different Ni/Co mass ratios in bimetallic Ni-Co/Al_2O_3. They found that the bimetallic catalyst with Ni/Co mass ratio of 2:1 generated the highest H_2 yield and CH_4 conversion (Tab. 2). Zolghadri et al. [113] achieved very high activity and stability by incorporating also Ce in the catalyst and synthesizing a Ni(10wt %)-Co(10wt %)-Ce(1wt %)/Al_2O_3 (Tab. 2). The latter researchers argued that by adding Ce there was an increase in Ni and Co dispersion, in their interaction with alumina and in the Brunauer-Emmett-Teller (BET) surface area.

Ce was used as a dopant of Ni(20wt %)/Al_2O_3 in two recent studies [116, 117]. In both reports Ce improved the dispersion of Ni and suppressed the formation of coke, resulting in catalysts with higher activity and stability than the unpromoted ones. Meshksar et al. [117] investigated the effect of Ce loadings of 1.5 and 3 wt % and found that the most active catalyst was the one with 1.5 wt % Ce. The increases Ce loading resulted in agglomeration of Ni and Ce particles, decreasing the activity. Khosravani et al. [116] tested a wider range (1.5–4.5 wt %) to find out that higher activity and stability belonged to the catalyst with 3 wt % Ce. Both catalysts activities can be seen in Tab. 2.

Several types of deposited carbon can be found on the used catalyst surfaces depending on the kind of feed and on the reforming conditions. Three main categories distinguish the kinds of deposited carbon based on the temperature under which they undergo oxidation: polymeric or monoatomic, filamentous and graphitic carbon [35, 118]. Polymeric and monoatomic carbon deposits require the least temperature to be oxidized, starting from 300 °C, filamentous carbon needs temperatures higher than 500 °C, and the graphitic carbon can be oxidized above 650 °C [35, 118].

Großmann et al. [118] studied the carbon formation on the surface of the three different catalysts, two nickel-based and one rhodium-based catalysts. They experimented with SMR at S/C ratios of 0 and 0.1 and at reaction temperatures between 450 °C and 500 °C. Main carbonaceous species found on the nickel catalysts were of filamentous nature whereas on the noble metal catalyst two different types of carbon were found with monoatomic or polymeric structure and at much lower amount. The nickel catalysts deactivated within several minutes at S/C = 0 and within a few hours at S/C = 0.1. The measured lifetime of the noble metal catalyst was approximately 100 times higher than that for the two nickel-based catalysts.

3.2 Ceria-Supported Catalysts

Ceria has been studied extensively studied as a promoting agent of the supports of the catalysts used for dry, steam, and autothermal reforming of methane and other organic substances. As a catalyst support material, it seems promising in limiting the deactivation by coking, due to its high oxygen storage capacity since oxygen takes part in the in-situ oxidation of carbonaceous species on the surface of the catalyst [122–128]. Ceria contributes to the adsorption and sequential dissociation of water molecules to –O and to –HO. The decomposition of H_2O on the support surface provides active oxygen, which diffuses through ceria. These oxygen species oxidize any carbon deposited on the surface of the catalyst, forming CO, CO_2, and H_2 [129]. The latter characteristic enhances the catalytic stability and H_2 yield.

Many researchers also employed mixed oxides of CeO_2 and ZrO_2. Addition of ZrO_2 to CeO_2 results in a support with high oxygen mobility and thermal stability [125, 127]. Liu et al. [130] studied the production of hydrogen thermodynamically and experimentally through methane steam and oxidative

 © 2023 The Authors. ChemBioEng Reviews published by Wiley-VCH GmbH

21969744, 0, Downloaded from https://onlinelibrary.wiley.com/doi/10.1002/cben.202300007 by Karlsruher Institution F. Technologie, Wiley Online Library on [26/07/2023]. See the Terms and Conditions (https://onlinelibrary.wiley.com/terms-and-conditions) on Wiley Online Library for rules of use; OA articles are governed by the applicable Creative Commons License

reforming on a Ni(12wt %)/Ce-ZrO_2/θ-Al_2O_3. Their catalyst showed very high activity and approached the equilibrium conversion of CH_4. In addition, the catalyst had a very long lasting stability (Tab. 3).

Roh et al. [122] used a similar catalyst for SMR at 600 °C with varying ratio of CeO_2/ZrO_2. The best catalyst was the Ni(15wt %)/$Ce_{0.8}Zr_{0.2}O_2$, which exhibited the highest conversion of methane and was the most stable during TOS due to high oxygen capacity. The same analogy of supports for a 15 wt % Ni-based catalyst was employed by Min-Ju Park et al. [131] for bireforming. They reported maximum a H_2 yield at 700 °C. Above 700 °C sintering of the catalyst was apparent and thus deactivation. Excess steam, i.e., higher S/CH_4 ratios, promoted methane conversion but decreased H_2 yield. They concluded that excess steam resulted in the SMR reaction being dominant over DRM and that the use of biogas as feed requires low S/CH_4 ratios. Their optimum S/CH_4 ratio was 1 (Tab. 3).

Goula et al. [123] compared the catalytic performance of a 8 wt % Ni catalyst supported on CeO_2-ZrO_2, with a Ni catalyst supported on ZrO_2 and an another on La_2O_3-ZrO_2 at biogas dry reforming. These catalysts are referred simply as Ni/Zr, Ni/CeZr, and Ni/LaZr. The latter two reached higher CH_4 and CO_2 conversions than the Ni/Zr. The H_2/CO ratio was higher for Ni/LaZr and Ni/Zr than for Ni/CeZr for low temperatures, but at higher temperatures it reached for Ni/CeZr and Ni/LaZr a similar value higher than the respective for Ni/Zr. Ni/CeZr had better stability than the other catalysts. Their results from the H_2-TPR indicated that the oxygen storage capacity and its lability followed the order: CeZr >> LaZr ≥ Zr.

Makri et al. [124] reported a bifunctional mechanism regarding DRM on Ni/$Ce_{1-x}Zr_xO_{2-\delta}$. This mechanism considers CH_4 activation as the rate-determining step that takes place on the Ni surface, while CO_2 activation occurs both on Ni and on oxygen vacancies at the Ni-support interface. Therefore, a big amount of labile oxygen ions and of oxygen vacancies on the support have a significant effect on catalytic activity and stability.

Angeli et al. [132] developed 10 wt % Ni and 1 wt % Rh catalysts supported on La_2O_3-ZrO_2 and La_2O_3-CeO_2-ZrO_2 for steam methane and biogas reforming at low temperatures in the range of 400–550 °C. The most active and stable catalyst was the Ni supported on La_2O_3-CeO_2-ZrO_2, which had almost stable CH_4 conversion during 90 h on stream (Tab. 3). They reported also that La_2O_3 contributes to the inhibition of coke formation as well, through the reaction of $La_2O_2CO_3$ with the deposited carbon. They observed the formation of amorphous carbon in contact with the Ni particles. For the Rh-based spent catalyst, only some scarce parts that were not in contact with the Rh particles were observed. Therefore, the loss of activity for the Rh-based catalyst might have been due to changes in the oxidation state of the metal nanoparticles. They also reported that the carbon, which had been formed, could be easily removed by hydrogenation, utilizing a part of the produced hydrogen.

Ceria has been compared to alumina as more suitable Pd catalyst support in the steam reforming of hydrocarbon fuels and the first exhibited higher hydrocarbons conversion rates for most reactions [133]. $CeZrO_2$-Al_2O_3 supports with different composition for Pd-Rh metals were studied at biogas steam reforming by Roy et al. [134]. High CH_4 conversions were found for all tested catalysts with a very small increase in the conversion with increased $CeZrO_2$ content. Only the catalyst without any $CeZrO_2$ performed dramatically worse for the entire range of tested temperature. A higher $CeZrO_2$ content in the alumina support resulted in reduced coke formation. All the catalysts maintained steady performances with insignificant changes for 200 h on stream, thus the inhibition of catalyst deactivation was not attributed to the $CeZrO_2$ addition. Sintering of the metal particles had taken place. Sintering of Rh particles on a CeO_2 and on a combined CeO_2-Al_2O_3 support could be inhibited if the catalysts are prepared in forms of nanorods and nanocubes [127]. In a similar way, ceria and zirconia seemed to inhibit the aggregation of Ni nanoparticles through intense interaction of Ni with those two oxides [128].

Sepehri and Rezaei [135] compared four catalysts, a Ni(25wt %)/Al_2O_3 catalyst and a Ni(25wt %)/Al_2O_3-CeO_2,with different contents of ceria (1, 3, and 6 wt %), in autothermal reforming of methane. It was found that the Ni catalyst with a ceria content of 3 wt % exhibited higher activity (Tab. 3) than the other catalysts with 1 and 6 wt % Ce-Al_2O_3 and higher resistance to coke deposition. It was also found that Ni supported on CeO_2-Al_2O_3 [136] and on gadolinium-doped ceria [137] could convert light hydrocarbons higher than methane to H_2, CO_2, CO, and CH_4, even at low temperatures in the range of 400–500 °C and high pressures of 8.5 and 30 bar.

Dan et al. [125] compared also the effects of addition of CeO_2 and La_2O_3 on 7 wt % Ni catalysts for SMR. Turnover frequency and CH_4 conversion followed this series for both high and low temperatures: Ni/Ce-Al > Ni/La-Al. At 700 °C, Ni/La-Al was progressively deactivating, while Ni/Ce-Al was very stable. Tab. 3 presents the data for the Ni/Ce-Al catalyst. Addition of CeO_2 to the Ni/Al catalysts resulted in the formation of porous amorphous carbon instead, whereas the addition of La_2O_3 led to graphitic carbon. For Ni/Ce-Al, there is a presence of Ce^{3+} ions at the CeO_2 surface. These ions enhance the adsorption of H_2O and its dissociation, generating a supplementary afflux of oxygenated species to the metal surface, which react with adsorbed CH_x inhibiting the formation of stable, crystalline carbon deposits.

The effect of cerium is dependent on the preparation method of the catalyst because it affects the dispersion of the active metal and the metal support interaction. In this way, the large surface area and stability of γ-Al_2O_3 is combined with the oxygen storage and release capability of CeO_2, as Luisetto et al. [138] argued. These researchers studied different catalyst preparation techniques of Ni(10wt %)/Al_2O_3-CeO_2 and their performances on DRM. The methods applied were coprecipitation, wet impregnation, sol gel and citric acid methods. Their abbreviations are, respectively, CP, WI, SG, and CA. The catalytic activity depended strongly on the preparation method. At 600 °C the activity of the catalysts prepared by the aforementioned methods followed this sequence: SG < WI < CA < CP whereas at 800 °C the sequence of activity was the following: WI < SG << CA < CP. Highest CH_4 conversion was obtained for the catalyst prepared by CP (Tab. 3).

Santander et al. [129] and Bao et al. [139] utilized this method as well, preparing catalyst supports with the incorporation of MgO. The addition of magnesium oxide improves the

These are not the final page numbers! ↗↗

21969744, 0, Downloaded from https://onlinelibrary.wiley.com/doi/10.1002/cben.202300007 by Karlsruher Institution F. Technologie, Wiley Online Library on [26/07/2023]. See the Terms and Conditions (https://onlinelibrary.wiley.com/terms-and-conditions) on Wiley Online Library for rules of use; OA articles are governed by the applicable Creative Commons License

Table 3. Catalysts for hydrocarbons reforming based on Ce-containing supports and their performance in terms of hydrocarbons conversion and H_2 yield, not only initially but also after TOS. The conditions to which each catalyst was subjected are also recorded, i.e. temperature, feed and space velocity. The pressure was in all cases atmospheric unless otherwise specified.

Type	Temp. [°C]	Feed ratio	TOS [h]	Space velocity	Hydrocarbons conversion [%]		H_2 yield [%]		Ref.
					Initial	After TOS	Initial	After TOS	
Ni(15wt %)/ $Ce_{0.8}Zr_{0.2}O_2$	600	S/CH_4 (1:1)	6	155426 h^{-1}	60	55–60	–	–	[122]
Ni(8wt %)/ CeO_2-ZrO_2	800	CH_4/CO_2 (1.5:1)	30	120 L g_{cat}^{-1} h^{-1}	60	60	43	36	[123]
Ni(7wt %)/ CeO_2-Al_2O_3	700	S/CH_4 (4:1)	48	3 L g_{cat}^{-1} h^{-1}	100	100	–	–	[125]
Rh(5wt %)/CeO_2	630	S/PG[a)] (3.5:1)	100	94 L g_{cat}^{-1} h^{-1}	100	100	–	–	[127]
Ni(12wt %)/ CeO_2-ZrO_2-SBA-15	630	S/PG (3.5:1)	30	94 L g_{cat}^{-1} h^{-1}	99	99	–	–	[128]
Ni(7wt %)/ CeO_2-MgO	600	S/C_2H_5OH (3:1)	18	4.9 L g_{cat}^{-1} h^{-1}	100	100	–	–	[129]
Ni(12wt %)/ $CeZrO_2$-θ-Al_2O_3	645	S/CH_4 (2.98:1)	200	1.25 L_{CH4} g_{cat}^{-1} h^{-1}	85–90	85–90	100	100	[130]
Ni(15wt %)/$CeZrO_2$	700	$S/CH_4/CO_2$ (3:3:2)	25	18.2×10^4 h^{-1}	90	90	89	89	[131]
Ni(10wt %)/ LaO_2-CeO_2-ZrO_2	500	S/CH_4 (1.5:1)	90	3×10^4 h^{-1}	16[b)]	16	–	–	[132]
Rh(1wt %)/ LaO_2-CeO_2-ZrO_2	500	S/CH_4 (1.5:1)	90	3×10^4 h^{-1}	14[b)]	10	–	–	[132]
Pd-Rh(1.31wt %)/ $CeZrO_2$-Al_2O_3	800	S/CH_4 (1.5:1)	200	1400 h^{-1}	96	96	–		[134]
Ni(25wt %)/ CeO_2-Al_2O_3	700	S/CH_4 (1:3)	20	22 L g_{cat}^{-1} h^{-1}	70	70	–		[135]
Ni(13wt %)-Ce(1.02wt %)/Al_2O_3	480–580–850*[3]	$S/(C_5–C_8)$ (2.7:1)	300	6000 h^{-1}	73[c)]	73	–	–	[136]
	750	S/CH_4 (3:1)	10	10000 h^{-1} (CH_4)	0.19 L $g^{-1}min^{-1}$ [c)]	0.19 L $g^{-1}min^{-1}$	–	–	[136]
Ni(19.5wt %)-Ru(0.05wt %)/ CGO[d)]	450	$S/(C_2–C_5)$ (3:1)	900	5000 h^{-1}	100	99	–	–	[137]
Ni(10wt %)/ CeO_2-Al_2O_3	800	CH_4/CO_2 (1:1)	5	9 L g_{cat}^{-1} h^{-1}	75	75	–	–	[138]
Ni(15wt %)/ CeMgAl	750	CH_4/CO_2 (0.96:1)	100	4.8×10^4 h^{-1}	94	88	–	–	[139]
			–	2.4×10^4 h^{-1}	98	–	85	–	[139]
Ni(10wt %)/ $Ce_{0.95}Mn_{0.05}O_2$	700	CH_4/CO_2 (1:1)	5	12 L g_{cat}^{-1} h^{-1}	70 (CP)[e)] 47 (SG)	60 (CP) 47 (SG)	–	–	[144]

[a)]PG: propylene glycol; [b)]Angeli et al. conducted stability tests at severe conditions for a model biogas feed, where the pressure was 7 bar, SG: sol-gel; [c)]Yang et al. (2016) evaluated their catalyst at 30 bar for its activity in hydrocarbons steam reforming. For their steam methane reforming experiments, the temperature of the catalytic bed at its entrance was 480 °C, at its point where its length was 2/3 of its total length was 580 °C and at its exit 850 °C. They also reported the activity of the catalyst in terms of converted volume of methane per unit of time and mass, i.e. mL/g/min; [d)]CGO: ceria doped with gadolinium, their catalytic experiments were at 8 bars; [e)]Different stabilities depending on the catalyst preparation method; CP: coprecipitation.

 © 2023 The Authors. ChemBioEng Reviews published by Wiley-VCH GmbH

21969744, 0, Downloaded from https://onlinelibrary.wiley.com/doi/10.1002/cben.202300007 by Karlsruher Institution F. Technologie, Wiley Online Library on [26/07/2023]. See the Terms and Conditions (https://onlinelibrary.wiley.com/terms-and-conditions) on Wiley Online Library for rules of use; OA articles are governed by the applicable Creative Commons License

oxygen storage capacity and mobility in the support, leading to lower carbon deposition rate [140–143]. Mousavi et al. [144] added Mn into the structure of a CeO_2 support for a 10 wt % Ni-based catalyst used for DRM. They reported that the addition of Mn into ceria enhances the redox behavior of the latter oxide, increases the oxygen mobility and the resistance against carbon formation. The coprecipitation method resulted in the highest CH_4 conversion among other methods, i.e., sol-gel and hydrothermal method. However, it is worth noting that after TOS the catalyst prepared by coprecipitation had a reduction in CH_4 conversion as opposed to the other one prepared by the sol-gel method, which resulted in stable catalytic performance.

Borges et al. [145] combined ceria and silica in different compositions and tested the resulted supports of a 10 wt % Ni-based catalyst at steam reforming of propane. Through the BET method, they reported higher specific surface area and smaller Ni crystallite size with increasing silica content. The catalyst with the higher conversion, around 75 % of propane and no deactivation after 25 h on stream, had a CeO_2:SiO_2 molar ratio of 75:25. The catalysts described before are listed in Tab. 3.

3.3 Silica-Supported Catalysts

Silica dioxide has been used recently as a Ni catalyst support for methane reforming [146–148] and for ethanol steam reforming [149]. Silica fibers (SFs) have been used recently as a catalyst support material. In the study of Mhadmhan et al. [149], the Ni(11wt %)/SF catalyst was used for ethanol steam reforming and had an almost complete conversion of ethanol at 500 °C whereas the Ni(11wt %)/SiO_2 catalyst reached complete conversion at 700 °C (Tab. 4). They reported also different performances of the catalysts based on various preparation methods of the supports: impregnation, deposition precipitation, and strong electrostatic adsorption. The Ni/SF, prepared by the latter method, had the highest ethanol conversion since it had smaller Ni particle sizes and higher dispersion. Amorphous carbon had widely covered the active sites of the Ni/SF catalyst prepared by impregnation whereas filamentous carbon formed on the one prepared by strong electrostatic adsorption. Ni nanoparticles were located on the carbon filaments and thus the activity of the catalyst prepared by strong electrostatic adsorption had not been affected as much as that of the one prepared by impregnation.

Silicon carbide is another type of support, which has been studied in heterogeneous catalysis due to its high thermal conductivity, high mechanical strength, low specific weight, and chemical inertness. Nevertheless, it has a low specific surface area [150, 151]. Palma et al. [150] used a ceria/alumina-based slurry as a wash coating means to increase the specific surface area of a 5 wt % Ni catalyst supported on silicon carbide; its performance is reported in Tab. 4.

Other forms of silica which have been used are the SBA-15, the acronym for Santa Barbara-15 [126, 128, 152] and MCM-41, the acronym for Mobil Oil Corporation-41 [153], which are two different types of mesoporous forms of silica. SBA-15 and MCM-41 have a high specific surface area, well-ordered hexagonal structure, and large pore volume [126, 153]. More specifically, SBA-15 can maintain the dispersion of active metal nanoparticles by confining them in its pore channels and it can also provide high thermal stability [128]. MCM-41, on

Table 4. Catalysts for hydrocarbons reforming based on silica supports and their performance in terms of hydrocarbons conversion and H_2 yield, not only initially but also after TOS. The conditions to which each catalyst was subjected are also recorded, i.e. temperature, feed and space velocity. The pressure was in all cases atmospheric.

Type	Temp. [°C]	Feed ratio	TOS [h]	Space velocity or residence time	Conversion of hydrocarbons [%]		H_2 yield [%]		Ref.
					Initial	After TOS	Initial	After TOS	
Ni/Y-SBA-15 (Ni/Si molar ratio = 0.1)	800	CH_4/CO_2 (1:1)	6	15×10^3 h^{-1}	58	50	–		[126]
Ni(12wt %)/CeO_2-ZrO_2-SBA-15	630	S/propylene glycol (3.5:1) Air/PG (0.15:1)	30	94 L $g_{cat}^{-1}h^{-1}$	98–99	98–99	–	–	[128]
Ni(12wt %)/CeO_2-ZrO_2-SBA-15	630		30	94 L $g_{cat}^{-1}h^{-1}$	98–99	98–99	–	–	[128]
Ni(5wt %)/SiO_2	750	S/CH_4 (1:1)	60	60 L $g_{cat}^{-1}h^{-1}$	–	–	90	90	[146]
Ni(5wt %)/Ce-SiO_2	750	$CH_4/CO_2/O_2$ (1.5:1:0.25)	100	66.432 L $g_{cat}^{-1}h^{-1}$	80	80	–		[147]
Ni(26wt %)/SiO_2-Al_2O_3	900	S/CH_4 (4:1)	–	$2.1\times10^4h^{-1}$	98–100	–	–		[148]
Ni(11wt %)/SF-SEA[a)]	600	S/EtOH (9:1)	16	18 $g_{cat}h$ mol^{-1} [b)]	100	100	65	65	[149]
Ni(5wt %)/CeO_2-SiC	700	S/CH_4 (3:1)	–	10^5h^{-1}	73	–	–		[150]
Ni/Y_2O_3-MgO-MCM-41	750	CH_4/CO_2 (1:1)	20	12 L $g_{cat}^{-1}h^{-1}$	79	75	–		[153]

[a)]SF: silica fibres; SEA: strong electrostatic adsorption; [b)]W/F_{A0}: catalyst mass/inlet molar flow rate of EtOH in $g_{cat}h$ mol^{-1}.

These are not the final page numbers! ↗↗

21969744, 0, Downloaded from https://onlinelibrary.wiley.com/doi/10.1002/cben.202300007 by Karlsruher Institution F. Technologie, Wiley Online Library on [26/07/2023]. See the Terms and Conditions (https://onlinelibrary.wiley.com/terms-and-conditions) on Wiley Online Library for rules of use; OA articles are governed by the applicable Creative Commons License

the other hand, is preferred for industrial applications due to its low-temperature synthesis [153].

3.4 Catalysts with Spinel Structure

Supports that are based on the aluminum spinel group have been mentioned in the literature for reforming applications. They consist mainly of Mg ($MgAl_2O_4$) or Zn ($ZnAl_2O_4$). A spinel structure that can be also found in those applications is the $NiAl_2O_4$ and its effect on the catalyst performance is discussed further [99, 119, 120, 127].

Habibi et al. [154] studied the effect of Ni addition in $MgAl_2O_4$ spinel for biogas dry reforming implementing a novel sol-gel method for the preparation of the catalysts without a surfactant. The best catalyst by means of reforming activity was the one with the highest Ni content, i.e., the $Mg_{0.8}Ni_{0.2}Al_2O_4$ (Tab. 5). With the Ni addition, they reported a strong metal support interaction due to the formation of $NiAl_2O_4$ spinel and due to the formation of the NiO-MgO solid solution. The formation of the latter solid solution contributed to the thermal stability of the catalyst.

Khani et al. [155] compared three different metals, namely, Ni, Pt, and Ru, with 3 wt % loading supported on $ZnLaAlO_4$ for DRM, SMR, and combined reforming of CH_4. The greatest catalytic activity and stability were reported for Ru/$ZnLaAlO_4$ and the worst for Pt/$ZnLaAlO_4$ (Tab. 5). They also reported that the $ZnLaAlO_4$ supported catalysts could be reduced by H_2 at much lower temperatures and that their H_2 consumption was less compared to that of Ni/Al_2O_3.

Another team [156] studied the addition of Pt to Ni(15wt %)/$MgAl_2O_4$. The addition of the noble metal on Ni catalysts increased Ni dispersion over the catalyst support and enhanced the reducibility of the catalyst. The catalytic activity increased with raise in Pt doping until 0.1 wt % (Tab. 5). Further addition of Pt led to a decrease in catalytic activity. An increase of Pt content up to 0.1 wt % reduced the particle size of the active metals, but further Pt addition raised it. Alloys formed by the noble metal and nickel decrease the formation of unreactive metal complexes, such as $NiAl_2O_4$ and reduce the carbon formation over the catalyst surface.

High calcination temperatures, e.g., 900 °C, can result also in the formation of the $NiAl_2O_4$ spinel [99]. This spinel phase is difficult to activate/reduce due to its thermal stability [120].

Table 5. Catalysts for hydrocarbons reforming based on spinel supports and their performance in terms of hydrocarbons conversion and H_2 yield, not only initially but also after TOS. The conditions to which each catalyst was subjected are also recorded, i.e. temperature, feed and space velocity. The pressure was in all cases atmospheric, unless otherwise specified.

Type	Temp. [°C]	Feed ratio	TOS [h]	Space velocity	Hydrocarbons conversion [%]		H_2 yield [%]		Ref.
					Initial	after TOS	Initial	after TOS	
Ni(7.5wt %)/ $NiAl_2O_4$-γ-Al_2O_3	850	CH_4/CO_2 (1.5:1), S/C (1:1)	0.5	850 h^{-1}	98–100	98–100	60	60	[119]
$Mg_{0.8}Ni_{0.2}Al_2O_4$	700	CH_4/CO_2 (1:1)	13.3	18 L $g_{cat}^{-1}h^{-1}$	75	70–75	–	–	[154]
Ru(3wt %)/ $ZnLaAlO_4$	700	S/CH_4 (3:1)	30	10500 h^{-1}	95–97	95–97	78–79	78–79	[155]
		CH_4/CO_2 (1:1)			68–70	68–70	60	60	
Pt(0.1wt %)- Ni(15wt %)/$MgAl_2O_4$	600	S/CH_4 (5:1)	8	0.34 $g_{cat}h\ mol_{CH4}^{-1}$ a)	67 (1 atm)	67 (1 atm)	–	–	[156]
					53 (10 atm)	45 (10 atm)	–	–	
Rh(1wt %)/$MgAl_2O_4$	600	S/$C_3H_8O_3$ (9:1)	18.6	35 L $g_{cat}^{-1}h^{-1}$	98	98	–		[157]
Ni(10wt %)-Ce/ $MgAl_2O_4$ (Ce/Ni molar ratio = 0.25)	700	$CH_4/H_2O/CO_2$ (1:0.8:0.4)	16	530 L $g_{cat}^{-1}h^{-1}$	81.3	–	–		[158]
Ni(12.5wt %)/ Ce(5wt %)-$ZnAl_2O_4$	700	CH_4/CO_2 (1:1)	8	18 L $g_{cat}^{-1}h^{-1}$	70	59–60	72.56	70.63	[159]
	750		–		78	–	88.54	–	[159]
Ni(10wt %)- Co(10wt %)- Ce(7wt %)/$MgAl_2O_4$	400	S/C_2H_6O (8.6:1)	–	60 L $g_{cat}^{-1}h^{-1}$	100	–	55	–	[161]
Ni(15wt %)- Co(5wt %)/$MgAl_2O_4$	700	S/CH_4 (1:1)	7	10 L $g_{cat}^{-1}h^{-1}$	83	83	–	–	[160]

a) W/F_{A0}: catalyst mass/inlet molar flow rate of methane $g_{cat}h\ mol^{-1}$.

21969744, 0, Downloaded from https://onlinelibrary.wiley.com/doi/10.1002/cben.202300007 by Karlsruher Institution F. Technologie, Wiley Online Library on [26/07/2023]. See the Terms and Conditions (https://onlinelibrary.wiley.com/terms-and-conditions) on Wiley Online Library for rules of use; OA articles are governed by the applicable Creative Commons License

However, $NiAl_2O_4$ may form an interfacial stabilizing layer for the formation of small size nickel particles with high dispersion and distribution across the support, inhibiting Ni sintering [119]. In the study of Tuna et al. [119], a Ni(7.5wt %)/$NiAl_2O_4$/γ-Al_2O_3 catalyst working at 850 °C demonstrated similar CH_4 conversion, H_2 yield, and H_2/CO ratio with a Ru(3.1wt %)/γ-Al_2O_3 working at 700 °C, in a bireforming process under atmospheric pressure (Tab. 5). Carbon deposition on the Ni catalyst was considered insignificant.

Experiments of glycerol steam reforming on catalysts based on noble metals, i.e., Rh, Ru, Pt, and Ir, with 1 wt % loading, which are supported on $MgAl_2O_4$, from Senseni et al. [157], demonstrated the superiority of Rh as active catalytic metal over the rest ones. H_2 selectivity was found to be the highest for the Rh catalyst, followed by Ir, Ru, and at last by Pt. Rh had a high and stable glycerol conversion (Tab. 5), while the other catalysts were losing their activities. The next most stable found to be Pt/$MgAl_2O_4$ with its activity falling from 95 % to 76 % after 5 h on stream.

Addition of Ce on the Ni(10wt %)/$MgAl_2O_4$ may result in high dispersion of active metal, as Koo et al. [158] demonstrated. They found that there was an optimum Ce/Ni ratio of 0.25 that increased Ni metal dispersion and BET surface area. With Ce/Ni increasing, the interaction of metal with support was promoted. The catalyst with a ratio Ce/Ni = 0.25 performed better catalytically in combined DRM and SMR than the rest and had minimum carbon deposition because of its high Ni dispersion. Movasati et al. [159] studied the effect of Ce promotion on the $ZnAl_2O_4$ with Ni (12.5 wt %) being the active metal. They reported that Ce addition leads to activity and stability increase up to a point, where further increase results to aggregation of CeO_2 on the catalyst surface. Their optimal catalyst consisted of 5 wt % cerium and is listed in Tab. 5.

$MgAl_2O_4$ has been utilized as a support for bimetallic Ni-Co catalysts, with investigations indicating that the loading of Co has a significant impact on the catalytic activity of 15 wt % Ni/$MgAl_2O_4$ SMR [160]. As the amount of Co added to the catalyst increased, coke formation decreased and CH_4 conversion improved. Interestingly, the catalyst with 5 wt % demonstrated slightly higher CH_4 conversion than the one with 9 wt %; the activity of the former is given in Tab. 5. It was found that in the as-prepared fresh catalys, Ni and Co covered the Mg-deficient tetrahedral sites in $MgAl_2O_4$ lattice, forming $NiAl_2O_4$ and $CoAl_2O_4$, while the rest Ni had formed NiO particles. Upon reduction, Ni and Co were exsolved from the lattice, forming Ni–Co alloys on the catalytic surface. This process was influenced by the Co loading, with higher Co loading resulting in more Ni and Co particles on the catalyst surface that could be reduced at a lower temperature. The exsolved cluster of Ni and Co also provided a high metal support interaction, which contributed to the catalyst's performance.

3.5 CaO-Based Catalysts

CaO is used in steam/dry reforming catalysts due to its basicity and coke prevention [152, 162–164].

A catalyst based on 9.3 wt % Ni and supported on CaO-ZrO_2 was used for DRM in the study of Wang et al. [162]. Its catalytic activity reached approximately the conversion predicted from thermodynamic equilibrium and could remain almost steady after 50 h on stream (Tab. 6). The surface structure of the used catalysts depended on the CH_4/CO_2 feed ratio. At the lowest ratio value, the surface of the spent catalyst was free of carbon residuals with a specific morphology. With this ratio increasing, formation of whisker carbon and Ni aggregation had begun to take place. Carbon formed on top of those aggregates blocking the metal actives sites.

Lertwittayanon et al. [163] used Ni(10wt %)/α-Al_2O_3 catalysts promoted by $CaZrO_3$ perovskite nanoparticles for steam methane reforming experiments. Reduction of the promoted catalysts with H_2 resulted in large pores at the $CaZrO_3$ lattice by the release of oxygen atoms. More $CaZrO_3$ nanoparticles meant more oxygen vacancies, which in turn signified more sites for steam adsorption and dissociation.

Vizcaíno et al. [152] performed ethanol steam reforming experiments with 7 wt % Co and Ni catalysts modified by Mg and Ca and supported on a silica structure. Addition of Ca led to the lowest coke deposition. Best performance was evidenced for the Ni catalyst modified by Ca with complete and stable ethanol conversion after 50 h TOS. Charisiou et al. [164] compared the performance of an 8 wt % Ni catalyst supported on MgO-Al_2O_3 with an 8 wt % Ni catalyst supported on CaO-Al_2O_3 and with an unpromoted Ni(8wt %)/Al_2O_3 catalyst, at biogas dry reforming. Both promoted catalysts exhibited higher CH_4 and CO_2 conversions than the unpromoted nickel catalyst for temperatures ranging between 550 °C and 750 °C. Above 750 °C the opposite behavior was evident which may be attributed to the increased activity of the Ni/Al_2O_3 catalyst for methane decomposition. The addition of CaO to the support resulted also in smaller Ni particles than those on the unpromoted Al_2O_3 support. Tab. 6 summarises the results of these studies.

3.6 Yttria-Supported Catalysts

Supports with yttrium in different formulations have resulted in satisfying performances for SMR [165] and biogas dry reforming [126, 153, 166–175].

Li and Zhang [126] tested a Ni-based catalyst supported on Y-containing SBA-15 for DRM (Tab. 7). They used different molar ratios of Y/SBA-15 and a constant 10 wt % Ni loading. They found that the catalytic activity was not constantly increasing with Y content but it reached a maximum performance at the molar ratio Y/SBA-15 = 0.004. The behavior of this catalyst was attributed to its higher specific surface area, larger pore diameter, and smaller Ni particle size. The other three catalysts with Y/Si ratios of 0.02, 0.06, and 0.08 resulted in higher CH_4 conversion than that of CO_2, due to methane decomposition. Addition of Y has shown to increase methane decomposition on NiO/Y_2O_3 catalysts [176]. They concluded that the support of Y-SBA-15 could result in the formation of Ni particles with small size and that Y promoted the reduction of NiO, due to oxygen vacancies on the surface of the catalyst.

These are not the final page numbers! ↗↗

21969744, 0, Downloaded from https://onlinelibrary.wiley.com/doi/10.1002/cben.202300007 by Karlsruher Institution F. Technologie, Wiley Online Library on [26/07/2023]. See the Terms and Conditions (https://onlinelibrary.wiley.com/terms-and-conditions) on Wiley Online Library for rules of use; OA articles are governed by the applicable Creative Commons License

Table 6. Catalysts for hydrocarbons reforming based on Ca-containing supports and their performance in terms of hydrocarbons conversion and H_2 yield, not only initially but also after TOS. The conditions to which each catalyst was subjected are also recorded, i.e. temperature, feed and space velocity. The pressure was in all cases atmospheric.

Type	Temp. [°C]	Feed ratio	TOS [h]	Space velocity	Hydrocarbons conversion [%]		H_2 yield		Ref.
					Initial	After TOS	Initial	After TOS	
Ni(7wt %)/ CaO-SBA-15	700	S/C_2H_6O (3.7:1)	50	$22.3\times10^3 h^{-1}$	100	100	–	–	[152]
Co(7wt %)/ CaO-SBA-15	700		50		100	100	–	–	[152]
Ni(9.3wt %)/ CaO-ZrO_2	750	CH_4/CO_2 (1:2)	50	48 L $g_{cat}^{-1}h^{-1}$	95	93	–	–	[162]
Ni(9.3wt %)/ CaO-ZrO_2	750	CH_4/CO_2 (2:1)	50	48 L $g_{cat}^{-1}h^{-1}$	68	50	–	–	[162]
Ni(10wt %)/ $CaZrO_3$-α-Al_2O_3	700	S/CH_4 (3:1)	10	60 L $g_{cat}^{-1}h^{-1}$	65	67	3.5 mol mol_{CH4}^{-1}	3.2 mol mol_{CH4}^{-1}	[163]
Ni(8wt %)/ CaO-Al_2O_3	850	CH_4/CO_2 (1.5:1)	–	120 L $g_{cat}^{-1}h^{-1}$	67	–	35%	–	[164]

Muñoz et al. [168] evaluated a Ni/CeO_2/yttria-stabilized zirconia (Ni/CYSZ) and a Ni/$Ce_{0.15}Zr_{0.85}O_2$ (Ni/CZ), in DRM (Tab. 7). The initial CH_4 and CO_2 conversions of those catalysts were almost complete, and this was attributed to the coexistence of side reactions like reverse WGS and methane decomposition. Under more severe DRM conditions, the Ni/CZ catalyst could not perform due to the rapid coke formation, whereas the Ni/CYSZ had a decrease in CH_4 conversion. Formation of filamentous carbon nanotubes took place, upon which were the Ni particles. The placement of the Ni particles at the top of the filaments resulted in accessible active metal particles for the dry reforming reactions. The Ni particle size and dispersion were similar for those two catalysts. Therefore, this difference in the stability of those catalysts may arise from the enhanced ability of the CYSZ support to oxidize the carbon accumulated on its surface. They argued that the structure of the CYSZ support is the reason for this enhanced carbon oxidizing ability.

Fakeeha et al. [169] compared under conditions of DRM Ni/CYSZ catalysts with Ce loadings in the range 1–3 wt % with a Ni/yttria-stabilized zirconia (Ni(5wt %)/YSZ) catalyst. The Ni/CYSZ with Ce loadings of 2 and 3 wt % outperformed the reference Ni(5wt %)/YSZ catalyst in terms of initial activity (Tab. 7). The Ce-promotion contributed to larger Ni particle size and facilitated the NiO reduction, i.e., weakened the metal support interaction. The formation of carbon filaments on the Ce-promoted catalyst was evident, compared to the unpromoted. These findings led the authors to suspect that Ce addition promoted side reactions that generate carbon, such as methane decomposition. The authors point to a lack of sites that function as strong bases and the formation of a CeO_2-ZrO_2 solution resulting in the weakening of the redox reaction of Ce that ultimately releases oxygen:

$$Ce^{4+} - O - Ce^{4+} \rightarrow Ce^{3+} - \text{Vacancy} - Ce^{3+} + 1/2O_2 \quad (21)$$

On the one hand, oxygen vacancies act as adsorption sites of DRM reactants and on the other hand, released oxygen gasifies the adsorbed carbon, producing CO [166].

Świrk et al. [170] conducted DRM on Ni-Mg-Al double-layered hydroxides (Ni^{2+}/Mg^{2+} of 0.33), referred to as DLHNi, with different yttrium contents of 0.6 and 1.5 wt %. The double-layered hydroxides (DLHs) have the general chemical formula $[M^{II}_{1-x}M^{III}_x(OH)_2]^{x+}(A^{n-})_{x/n}\cdot mH_2O$, where M^{II} are the divalent cations of metal and M^{III} the trivalent ones, A^{n-} is a n-valent anion and m is the number of water molecules. The catalyst with the maximum CH_4 and CO_2 conversions was the one with the highest yttrium content (Tab. 7). This catalyst demonstrated the highest stability as well. By comparing their results with the ones from Li et al. [126], who prepared Ni/Y-SBA-15 catalysts (molar ratio of Ni/Si of 0.1), they suggested that their yttrium-modified DLHs could suppress more effectively the methane decomposition reaction. The extensive Ni dispersion and high specific surface area caused the high catalytic performance.

In one of their recent studies [171], where similar catalysts were employed but with Y contents of 3, 4, and 8 wt %, it was found that the most active catalyst in terms of CH_4 conversion was the one with 4 wt % Y content, which was related to the smallest Ni^0 particle size. Nevertheless, the most resistant catalyst to coke deposition was the DLHNi-$Y_{8.0}$ due to its improved Ni reducibility and strongest basicity. The reason for the lower activity of this catalyst lied in the formation of bigger Ni particles that cannot facilitate the DRM.

The same team tested Ce- and Y-promoted double-layered hydroxides, namely, DLHNiCe, DLHNiCe-$Y_{0.2}$, DLHNiCe$Y_{0.4}$, and DLHNiCe-$Y_{0.6}$ for DRM [172]. A decrease in CH_4 and CO_2 conversion for the DLHNiCe-$Y_{0.6}$ catalyst was found, compared with the other catalysts. Further tests on the best performing catalysts resulted in the following sequence in terms of CH_4 conversion: DLHNi < DLHNiCe-$Y_{0.4}$

21969744, 0, Downloaded from https://onlinelibrary.wiley.com/doi/10.1002/cben.202300007 by Karlsruher Institution F. Technologie, Wiley Online Library on [26/07/2023]. See the Terms and Conditions (https://onlinelibrary.wiley.com/terms-and-conditions) on Wiley Online Library for rules of use; OA articles are governed by the applicable Creative Commons License

< DLHNiCe$Y_{0.2}$ < DLHNiCe. The promotion with Ce rather than with Y [170] resulted in an increase of the basicity, i.e., formation of more strong basic sites, improved Ni dispersion, and smaller Ni crystallite size.

Wang et al. [173] tested the effect of Y addition on NiO-ZrO_m. The addition of Y on the catalyst resulted in smaller Ni particles and in increased amount of weak and medium-strong basic sites. These two characteristics contributed to reduced carbon deposition on the catalyst surface. Y enhanced the interaction between Ni and ZrO_m and subsequently the Ni dispersion. Nevertheless, the promoted NiO-ZrO_m-YO_n catalyst had lower specific surface area and smaller pore volume and its activity at DRM was lower than that of the NiO-ZrO_m.

Damyanova et al. [174] studied the dry reforming of methane on 10 wt % Ni- and 1 wt % Rh-based monometallic and bimetallic catalysts, supported on alumina oxide and on a Y-modified alumina support. The Y addition on the support increased the CH_4 conversion of the monometallic Ni catalyst. This was due to the increased agglomeration of Ni particles on the alumina support compared to the Y-modified support. Y-modified Ni/Al catalyst was more active than the Ni/Al. They suggested that the higher stability of Y-modified Ni/Al catalysts comes from the increased number of basic sites on the yttria-alumina support. These basic sites contribute to the formation of oxycarbonates via the interaction of Y_2O_3 species with CO_2, which in turn provide a plethora of active oxygen species for the oxidation of deposited carbon [167]. However, the bimetallic catalyst supported on alumina performed better, not only in terms of CH_4 conversion but of CO_2 as well. The Rh/Al was more stable than the Rh/Y-Al. Larger NiO species were observed on the RhNi/Y-Al than on the RhNi/Al catalyst, which are more difficult to reduce and might result in less dispersive Ni particles.

Supports that contained yttrium in pyrochlore form, perovskite, or in the form of MCM-41 have also drawn attention as catalysts for reforming processes [36]. Recently, Taherian et al. [153] tested Ni/MgO-MCM-41 catalysts promoted with Y_2O_3 with different concentrations of yttrium oxide. The concentration of 2 wt % Y_2O_3 resulted in a larger BET specific surface area and smaller active metal particle diameters than the other Y-promoted catalysts. The catalysts were evaluated at DRM, where the Y_2O_3-Ni/MgO-MCM-41 with 2 wt % Y_2O_3 was the

Table 7. Catalysts for hydrocarbons reforming based on Y-containing supports and their performance in terms of hydrocarbons conversion and H_2 yield, not only initially but also after TOS. The conditions to which each catalyst was subjected are also recorded, i.e., temperature, feed and space velocity. The pressure was in all cases atmospheric, unless otherwise specified.

Type	Temp. [°C]	Feed ratio	TOS [h]	Space velocity	Hydrocarbons conversion [%]		H_2 yield		Ref.
					Initial	After TOS	Initial	After TOS	
Ni/Y-SBA-15 (Ni/Si molar ratio = 0.1)[a)]	750	CH_4/CO_2 (1:1)	6	15 000 h^{-1}	56–57	50	–		[126]
Y_2O_3(2wt %)-Ni/MgO-MCM-41	750	CH_4/CO_2 (1:1)	20	12 L $g_{cat}h^{-1}$	79	75	–		[153]
Ni(5wt %)/Al_2O_3-YSZ*[1]	800	S/CH_4 (1.5:1)	–	13 649.7 h^{-1}	90	–	64 %	–	[165]
Ni/CeO_2-YSZ[b)]	750	CH_4/CO_2 (1:1)	70	60 L $g_{cat}h^{-1}$	80	60	–		[168]
Ni(5wt %)-Y(15wt %)-ZrO_2	700	CH_4/CO_2 (1:1)	7	42 L $g_{cat}h^{-1}$	–		67.5 %	63.7 %	[166]
Ni(5wt %)-Ce(2wt %)/YZ	700	CH_4/CO_2 (1:1)	7.6	42 L $g_{cat}h^{-1}$	85	76	–		[169]
Ni/Mg-Al-Y (1.5wt %) DLH[c)]	700	CH_4/CO_2 (1:1)	10	20 000 h^{-1}	75	75	–		[170]
Ni(23wt %)/Mg-Al-Ce-$Y_{0.2}$ DLH[c)]	700	CH_4/CO_2 (1:1)	5	20 000 h^{-1}	80	85	–		[172]
Rh(1wt %)Ni (10wt %)/Y_2O_3-Al_2O_3	550	CH_4/CO_2 (1:1)	5	120 L $g_{cat}h^{-1}$	46	46	30%	30%	[174]
Ni(5mol.%)/$SrYTiO_3$	750	CH_4/CO_2 (1:1)	100	60 000 h^{-1}	70	70	–		[175]
Ni(10wt %)/$Y_2Zr_2O_7$	800	S/CH_4 (2:1)	100 (1 atm)	72 L $g_{cat}h^{-1}$	100 (1 atm)	100 (1 atm)	–		[177]
			200 (20 atm)	18 L $g_{cat}h^{-1}$	65 (20 atm)	65 (20 atm)	–		

[a)]The molar ratio of Ni/Si was fixed at 0.1; [b)]YSZ: yttria-stabilized zirconia; Ni content was 0.04 mmol m^{-2} of support oxide; [c)]DLH: double-layered hydroxides; molar ratio of Ni^{2+}/Mg^{2+} 0.33.

 © 2023 The Authors. ChemBioEng Reviews published by Wiley-VCH GmbH

21969744, 0, Downloaded from https://onlinelibrary.wiley.com/doi/10.1002/cben.202300007 by Karlsruher Institution F. Technologie, Wiley Online Library on [26/07/2023]. See the Terms and Conditions (https://onlinelibrary.wiley.com/terms-and-conditions) on Wiley Online Library for rules of use; OA articles are governed by the applicable Creative Commons License

most active and stable (Tab. 7). The addition of 2 wt % yttria enhanced the reduction of Ni^{2+} to Ni^0. The authors argued that the one-pot synthesis is a method for catalyst preparation that can result in a uniform distribution of magnesium, nickel, and yttrium on the support surface.

Pyrochlores have a major drawback when they are prepared by regular methods, such as coprecipitation and sol-gel, because they result in low dispersion of Ni active sites [177]. Fang et al. [177] tested different preparation methods of those supports and found that the support prepared by glycine-nitrate combustion gave the highest conversion and was stable for a very long TOS (Tab. 7). Perovskites, on the other hand, provide very extensive dispersion of the active metals. Their general chemical formula is ABO_3, where A-site cation is in the lattice center and B-site ions at the lattice corners. The active metal particles are integrated in the position B of the chemical formula ABO_3 and inhibit the carbon formation [163, 178].

In this chapter, attention has been paid to catalysts for SMR. The most active ones, in terms of CH_4 conversion, were either Ni-based or based on Pd-Rh and Ru. The Ni-based ones were supported on CeO_2-Al_2O_3 or $Y_2Zr_2O_7$. Their operating temperatures ranged from 645 °C up to 800 °C and their S/C ratios from 2 up to 4. Their active metal loadings were in the range of 7–12 wt %. They achieved CH_4 conversions higher than 95 %. The ones based on noble metals were supported on $CeZrO_2$-Al_2O_3 and $ZnAl_2O_4$. They required much lower active metal loadings, i.e., 1.3 and 3 wt % and less steam than the Ni-based ones, at the same temperature. For example, the bimetallic Pd-Rh/CeO_2-Al_2O_3 was operated at 800 °C, like the Ni/$Y_2Zr_2O_7$, but at lower S/C ratio of 1.5, compared with the Ni/$Y_2Zr_2O_7$, with S/C = 2. Similarly, the Ru/$ZnAlO_4$, operated at 700 °C, required less steam, i.e., S/C = 3, than the Ni/CeO_2-Al_2O_3 which had an S/C of 4.

From the studied SMR catalysts, there were two catalysts with very high H_2 yields. These were the Ni(12wt %)/$CeZrO_2$-θ-Al_2O_3, used at 645 °C and S/C = 3, with a H_2 yield of 100 % and a Ni(5wt %)/SiO_2 used at 750 °C and S/C = 1, with a yield of 90 %. Although both catalysts resulted in high H_2 yields, the first one provided a slightly higher yield than the second one. This can be attributed to the higher S/C ratio and to the significantly lower GHSV of the first catalyst, which was 1.25 $L_{CH4}\,g_{cat}^{-1}h^{-1}$, compared to the second one with a GHSV of 60 $L_{CH4}\,g_{cat}^{-1}h^{-1}$.

The stability of the catalysts in SMR applications was also considered. Only those catalysts that were subjected to long-term experiments were included in this study. The longest experiment duration found was 200 h and was used for three catalysts: Ni(12wt %)/$CeZrO_2$-θ-Al_2O_3, Pd-Rh(1.31wt %)/$CeZrO_2$-Al_2O_3, and Ni(10wt %)/$Y_2Zr_2O_7$. All of them showed stable conversion of methane. Therefore, these two supports confer high and stable catalytic activity.

Catalysts for the DRM were also the focus of research in this chapter. The catalysts with the highest CH_4 conversion were a Ni(15wt %)/CeMgAl catalyst, used under 750 °C and CH_4/CO_2 ratio of 0.96, generating a CH_4 conversion of 98 %, and a Ni(9.3wt %)/CaO-ZrO_2 catalyst, used under the same temperature but lower CH_4/CO_2 ratio of 0.5, resulting in 95 % conversion of CH_4.

Higher methane concentrations are associated with more unfavorable conditions for the catalyst, since higher concentration of CH_4 can result in increased coke formation and loss of activity. Thus, the Ni(15wt %)/CeMgAl is considered as a more active catalyst in terms of CH_4 conversion and more resistant to deactivation. This is evidenced by the stability experiments, which showed a reduction in methane conversion from 94 % to 88 %, after 100 h of TOS. Slightly enhanced stability was observed for the Ni(5wt %)/$SrYTiO_3$, which showed no loss of its initial activity, which accounted for 70 % CH_4 conversion, under the same TOS, same temperature, and CH_4/CO_2 ratio.

The Ni(15wt %)/CeMgAl also produced hydrogen with very high yield, equal to 85 %. However, the catalyst with the highest H_2 yield was the Ni(12.5wt %)/Ce-$ZnAl_2O_4$, which under 750 °C and CH_4/CO_2 ratio of 1:1 resulted in a yield of 88.54 %.

The hydrocarbons higher than methane, mostly C_2–C_4 alkanes and alkenes, are by-products from the SCWG of biomass. The criteria for the selection of catalysts suitable for hydrocarbons steam reforming are their high conversion and their long-lasting stability, since the hydrocarbons have to be removed from the SCWG product gas before the SMR reactor. There were two catalysts effective in complete conversion of the hydrocarbons. The first one was a Ni(19.5wt %)-Ru(0.05wt %)/CGO, operated at 450 °C and with a feed of C_2–C_5 hydrocarbons with S/C ratio of 3. Apart from the complete conversion of hydrocarbons, this catalyst was stable for 900 h of TOS. A Rh(5wt %)/Al_2O_3 had also complete conversion of propane at 750 °C and S/C of 4, for 120 h. Long-lasting activity of 300 h was also reported for a Ni(13wt %)-Ce(1.02wt %)/Al_2O_3 catalyst, for a feed of C_5–C_8 with a S/C ratio of 2.7, nonetheless without very high activity of 73 %.

Although some more technologies and different feedstocks are reported here, their analysis goes beyond the scope of this review.

4 Conclusions

This literature review introduces the combined process of biomass gasification in supercritical water and reforming of the produced methane and the rest hydrocarbons. Hydrogen is the desired product of this process. Many studies of SCWG of organic resources have shown that the produced hydrogen is not only found in the form of H_2, but also bound to hydrocarbons and especially to CH_4. Therefore, a downstream process that will convert the hydrocarbons into H_2 and carbon oxides should be implemented to produce hydrogen from biomass. An important aspect of this work is the selection of the right catalysts, one for the SCWG step and the other for the subsequent step of steam/dry reforming.

Recent advances in the catalytic gasification of biomass with supercritical water highlight that the catalysts which offer high carbon gasification efficiency and hydrogen yield are those based on nickel with supports of magnesia, ceria, zirconia, and alumina or mixtures thereof. Other metals, like Co and Ru, can act as promoters of the Ni, since they have been found to increase the yield of H_2 and the total gas yield. These catalysts were found to promote extensively the steam methane reform-

21969744, 0, Downloaded from https://onlinelibrary.wiley.com/doi/10.1002/cben.202300007 by Karlsruher Institution F. Technologie, Wiley Online Library on [26/07/2023]. See the Terms and Conditions (https://onlinelibrary.wiley.com/terms-and-conditions) on Wiley Online Library for rules of use; OA articles are governed by the applicable Creative Commons License

ing reaction under 700–800 °C and 240–250 bar. Under low or moderate temperatures, i.e., 385–425 °C or 550–600 °C, respectively, and/or high pressure in the range 250–520 bar, high CGE, high CH_4 yield, and low yield of H_2 was provided by the Raney-nickel catalysts. These catalysts facilitate the C–C bond cleavage and promote the methanation. Other effective catalysts that acted similarly were the Ni/MgO, the Ni/ZrO_2, and the Ru supported on Al_2O_3 or TiO_2 or CeO_2.

The temperature range covered by the literature for biomass SCWG lies between 380 °C and 800 °C. Many studies work with glucose as model biomass compound. The transition to continuous processes with the aim to design catalysts with high activity and resistance to coke and tar formation should be an aspect of future research. Most of the literature regarding the SCWG of organic substances is based on batch processes. More specifically, all the studies that have used biomass resources as a feedstock concern batch processes with relatively short reaction times. Those data cannot provide information about the long-lasting stability of the SCWG catalysts. Prior to the catalytic biomass gasification and the reforming of hydrocarbons, gas-cleaning steps are necessary, so that any impurities that can deactivate the catalysts, like sulfur, are removed. A suitable material for that purpose is ZnO.

One process of reforming the hydrocarbons resulting from biomass gasification to convert them into hydrogen is steam reforming. The most suitable catalysts for this purpose are those that offer high activity, i.e., high methane conversion and hydrogen yield, and long-term stability. The most active catalysts with the highest stability had nickel or noble metals such as Ru or Pd-Rh as the active metal. The supports used for nickel were CeO_2-Al_2O_3, $CeZrO_2$-Al_2O_3, $Y_2Zr_2O_7$, and SiO_2, while the supports for the noble metals were correspondingly $CeZrO_2$-Al_2O_3 and $ZnAl_2O_4$. In addition to the steam reforming of methane, ceria, doped with gadolinium, was also used as a support for catalysts for the steam reforming of heavier hydrocarbons, offering stable complete conversion of C_2–C_5 hydrocarbons.

The second option for the catalytic treatment of the SCWG product gas is the dry reforming of methane, since CO_2 is also produced in a comparable amount with hydrogen and methane. The catalysts with the highest methane conversion and hydrogen yield in dry reforming were nickel-based and supported by CeO_2-MgO-Al_2O_3 or CaO-ZrO_2 or Ce-$ZnAl_2O_4$. These supports, together with the $SrYTiO_3$, provided the highest stability as well.

Ceria has been considered as a very promising support for catalysts in steam/dry reforming of methane. Its properties help in the oxidation of carbonaceous deposits on the surface of catalysts. Addition of other metal oxides, such as ZrO_2 or Al_2O_3 in the catalyst support can enlarge the surface area and enhance the overall oxygen mobility and thermal stability, reducing coke formation. CaO together with ZrO_2 or Al_2O_3 was used also as a support for steam and dry reforming of methane. Calcium offers an increase in the basicity of the catalyst and acts preventing coke formation.

In conclusion, the integrated SCWG reforming process option presents high potential to be applied for green hydrogen production from biomass. The plethora of catalytic formulations with promising performance in both process steps needs to be further fine-tuned towards minimization of activity loss in extended TOS evaluation in parallel with studies to optimize process variables and reactor configurations for continuous-flow operation using real biomass as feedstock.

Conflicts of Interest

The authors declare no conflict of interest.

Athanasios Vadarlis obtained a Master of Science (M.Sc.) in chemical engineering from the Aristotle University of Thessaloniki (AUTH) in 2019. He is currently a Ph.D. candidate at the Karlsruhe Institute of Technology (KIT) at the Department of Chemical and Process Engineering. He is conducting his research at the Institute of Catalysis Research and Technology (IKFT, KIT). His research focuses on process development and testing for hydrogen production from sustainable resources, supercritical water gasification of biomass and model compounds, and steam reforming of hydrocarbons. His research activity lies between the fields of process engineering and heterogeneous catalysis.

Sofia Angeli is a senior scientist in Karlsruhe Institute of Technology (Germany). She obtained her chemical engineering diploma in 2009, her Master degree in material science in 2012, and Ph.D. degree in 2016 at the Aristotle University of Thessaloniki (Greece). Her doctoral study was focused on intensified catalytic methane steam reforming processes. Her present research interests include catalysis in methane conversion processes, pollution control, and carbon dioxide utilization processes in terms of experiments and (micro)kinetic modeling.

 © 2023 The Authors. ChemBioEng Reviews published by Wiley-VCH GmbH

21969744, 0, Downloaded from https://onlinelibrary.wiley.com/doi/10.1002/cben.202300007 by Karlsruher Institution F. Technologie, Wiley Online Library on [26/07/2023]. See the Terms and Conditions (https://onlinelibrary.wiley.com/terms-and-conditions) on Wiley Online Library for rules of use; OA articles are governed by the applicable Creative Commons License

Angeliki Lemonidou is Professor of chemical engineering at the Aristotle University of Thessaloniki. She is Director of the Petrochemical Technology Lab and collaborating faculty member of CERTH/CPERI. She was Head of the Chemical Engineering School AUTH (2020–2022) and Vice President of EFCATS (2017–2019). Her research interests are in catalysis and reaction engineering aiming at the development of new materials and processes with minimum carbon footprint on natural gas valorization, biomass conversion, plastic chemical recycling, and carbon capture and utilization.

Nikolaos Boukis is expert in the field of supercritical water. He studied chemistry at the University of Athens (NKUA) (1976–1981). He received his Ph.D. from the University of Heidelberg in the fields of radiochemistry and physical chemistry (graduated in 1985). Since 1987 he is an academic employee of KIT. Since 1992 he has been leading application-oriented work in the field of supercritical water, in particular corrosion of the reactor material and biomass gasification and liquefaction. He is responsible for the pilot plant VERENA.

Jörg Sauer is full Professor and Director at the Institute of Catalysis Research and Technology (IKFT) at Karlsruhe Institute of Technology since 2012. His research interest includes the development and scale-up of process chains, new catalysts for the production of synthetic liquid fuels and chemicals based on renewable sources, process simulation and techno-economic evaluation of production processes, as well as the application of fuel components in internal combustion engines.

Acknowledgment

The research work that led to the writing of this review article is funded by the research project Helmholtz European Partnership for Technological Advancement (HEPTA), under grant agreement no. PIE-0016, which promotes research and development of advanced technologies in the research areas Climate, Energy, and Environment and more specifically in the topics "Air Quality", "Atmospheric Physics", "Biomass", and "Smart Cities". Open access funding enabled and organized by Projekt DEAL.

Symbols used

CGE	[%]	carbon gasification efficiency
p	[bar]	pressure
R_{Hb}	[%]	ratio of hydrogen bound in hydrocarbons to total produced hydrogen
RR_{CO}	[–]	stoichiometric coefficient of carbon monoxide from the reforming reactions of hydrocarbons
RR_{H2}	[–]	stoichiometric coefficient of hydrogen from the reforming reactions of hydrocarbons
T	[°C]	temperature
Y_i	[mol kg^{-1}]	yield of methane or hydrogen from the gasification of organic compounds in supercritical water
Y_{total}	[mol kg^{-1}]	yield of total product gas from the gasification of organic compounds in supercritical water

Greek letter

ΔH^{298K}	[kJ mol^{-1}]	enthalpy of chemical reaction at 298 K

Abbreviations

AC	activated carbon
BET	Brunauer-Emmett-Teller
BRM	bireforming
CA	citric acid
CGE	carbon gasification efficiency
CGO	ceria doped with gadolinium
CNT	carbon nanotube
CP	coprecipitation
CYSZ	ceria/yttria-stabilized zirconia
CZ	ceria-stabilized zirconia
DLH	double-layered hydroxide
DRM	dry reforming of methane
GHSV	gas hourly space velocity
HTL	hydrothermal liquefaction
MCM-41	Mobil oil corporation-41
PSA	pressure swing adsorption
PWS	paper waste sludge
SBA-15	Santa Barbara-15
SCW	supercritical water
SCWG	supercritical water gasification

 © 2023 The Authors. ChemBioEng Reviews published by Wiley-VCH GmbH

21963744, 0, Downloaded from https://onlinelibrary.wiley.com/doi/10.1002/cben.202300007 by Karlsruher Institution F. Technologie, Wiley Online Library on [26/07/2023]. See the Terms and Conditions (https://onlinelibrary.wiley.com/terms-and-conditions) on Wiley Online Library for rules of use; OA articles are governed by the applicable Creative Commons License

SF	silica fibers
SG	sol-gel technique
SMR	steam methane reforming
TOS	time-on-stream
WGS	water-gas shift
WI	wet impregnation

References

[1] S. Masoudi Soltani, A. Lahiri, H. Bahzad, P. Clough, M. Gorbounov, Y. Yan, *Carbon Capture Sci. Technol.* **2021**, *1*, 100003. DOI: https://doi.org/10.1016/J.CCST.2021.100003

[2] M. Erans, E. S. Sanz-Pérez, D. P. Hanak, Z. Clulow, D. M. Reiner, G. A. Mutch, *Energy Environ. Sci.* **2022**, *15 (4)*, 1360–1405. DOI: https://doi.org/10.1039/D1EE03523A

[3] U. S. Mohanty, M. Ali, M. R. Azhar, A. Al-Yaseri, A. Keshavarz, S. Iglauer, *Int. J. Hydrogen Energy* **2021**, *46 (65)*, 32809–32845. DOI: https://doi.org/10.1016/j.ijhydene.2021.07.097

[4] D. B. Pal, A. Singh, A. Bhatnagar, *Int. J. Hydrogen Energy* **2022**, *47 (3)*, 1461–1480. DOI: https://doi.org/10.1016/J.IJHYDENE.2021.10.124

[5] A. Arregi, M. Amutio, G. Lopez, J. Bilbao, M. Olazar, *Energy Convers. Manage.* **2018**, *165*, 696–719. DOI: https://doi.org/10.1016/j.enconman.2018.03.089

[6] J. D. Holladay, J. Hu, D. L. King, Y. Wang, *Catal. Today* **2009**, *139 (4)*, 244–260. DOI: https://doi.org/10.1016/j.cattod.2008.08.039

[7] L. Ferreira-Pinto, M. P. Silva Parizi, P. C. Carvalho de Araújo, A. F. Zanette, L. Cardozo-Filho, *Int. J. Hydrogen Energy* **2019**, *44 (47)*, 25365–25383. DOI: https://doi.org/10.1016/j.ijhydene.2019.08.023

[8] C. Rodriguez Correa, A. Kruse, *J. Supercrit. Fluids* **2018**, *133*, 573–590. DOI: https://doi.org/10.1016/j.supflu.2017.09.019

[9] C. S. Lee, A. V. Conradie, E. Lester, *Chem. Eng. J.* **2021**, *415*, 128837. DOI: https://doi.org/10.1016/j.cej.2021.128837

[10] L. Zhang, P. Champagne, C. Charles Xu, *Bioresour. Technol.* **2011**, *102 (17)*, 8279–8287. DOI: https://doi.org/10.1016/j.biortech.2011.06.051

[11] M. J. Sheikhdavoodi, M. Almassi, M. Ebrahimi-Nik, A. Kruse, H. Bahrami, *J. Energy Inst.* **2015**, *88 (4)*, 450–458. DOI: https://doi.org/10.1016/J.JOEI.2014.10.005

[12] M. Shahbaz, T. Al-Ansari, M. Aslam, Z. Khan, A. Inayat, M. Athar, S. R. Naqvi, M. A. Ahmed, G. McKay, *Int. J. Hydrogen Energy* **2020**, *45 (30)*, 15166–15195. DOI: https://doi.org/10.1016/J.IJHYDENE.2020.04.009

[13] J. Yanik, S. Ebale, A. Kruse, M. Saglam, M. Yüksel, *Int. J. Hydrogen Energy* **2008**, *33 (17)*, 4520–4526. DOI: https://doi.org/10.1016/J.IJHYDENE.2008.06.024

[14] A. G. Chakinala, D. W. F. Brilman, W. P. M. Van Swaaij, S. R. A. Kersten, *Ind. Eng. Chem. Res.* **2010**, *49 (3)*, 1113–1122. DOI: https://doi.org/10.1021/ie9008293

[15] P. Azadi, S. Khan, F. Strobel, F. Azadi, R. Farnood, *Appl. Catal., B* **2012**, *117–118*, 330–338. DOI: https://doi.org/10.1016/j.apcatb.2012.01.035

[16] J. Louw, C. E. Schwarz, A. J. Burger, *Bioresour. Technol.* **2016**, *201*, 111–120. DOI: https://doi.org/10.1016/j.biortech.2015.11.043

[17] N. Boukis, W. Habicht, G. Franz, E. Dinjus, *Mater. Corros.* **2003**, *54 (5)*, 326–330. DOI: https://doi.org/10.1002/maco.200390072

[18] Y. Matsumura, T. Minowa, B. Potic, S. R. A. Kersten, W. Prins, W. P. M. Van Swaaij, B. Van De Beld, D. C. Elliott, G. G. Neuenschwander, A. Kruse, et al., *Biomass Bioenergy* **2005**, *29 (4)*, 269–292. DOI: https://doi.org/10.1016/j.biombioe.2005.04.006

[19] D. C. Elliott, L. J. Sealock, E. Baker, *Ind. Eng. Chem. Res.* **1994**, *33 (3)*, 558–565. DOI: https://doi.org/10.1021/ie00027a012

[20] D. C. Elliott, T. R. Hart, G. G. Neuenschwander, L. J. Rotness, M. V. Olarte, A. H. Zacher, *Ind. Eng. Chem. Res.* **2012**, *51 (33)*, 10768–10777. DOI: https://doi.org/10.1021/ie300933w

[21] D. C. Elliott, *Biofuels Bioprod. Biorefining* **2008**, *2 (3)*, 254–265. DOI: https://doi.org/10.1002/bbb.74

[22] M. H. Waldner, F. Krumeich, F. Vogel, *J. Supercrit. Fluids* **2007**, *43 (1)*, 91–105. DOI: https://doi.org/10.1016/J.SUPFLU.2007.04.004

[23] A. A. Peterson, F. Vogel, R. P. Lachance, M. Fröling, M. J. Antal, J. W. Tester, *Energy Environ. Sci.* **2008**, *1 (1)*, 32–65. DOI: https://doi.org/10.1039/B810100K

[24] G. Peng, C. Ludwig, F. Vogel, *ChemCatChem* **2016**, *8 (1)*, 139–141. DOI: https://doi.org/10.1002/CCTC.201500995

[25] A. G. Haiduc, M. Brandenberger, S. Suquet, F. Vogel, R. Bernier-Latmani, C. Ludwig, *J. Appl. Phycol.* **2009**, *21 (5)*, 529–541. DOI: https://doi.org/10.1007/S10811-009-9403-3/FIGURES/4

[26] S. Stucki, F. Vogel, C. Ludwig, A. G. Haiduc, M. Brandenberger, *Energy Environ. Sci.* **2009**, *2 (5)*, 535–541. DOI: https://doi.org/10.1039/B819874H

[27] M. Schubert, J. W. Regler, F. Vogel, *J. Supercrit. Fluids* **2010**, *52 (1)*, 113–124. DOI: https://doi.org/10.1016/J.SUPFLU.2009.10.003

[28] G. Peng, F. Vogel, D. Refardt, C. Ludwig, *Ind. Eng. Chem. Res.* **2017**, *56 (21)*, 6256–6265. DOI: https://doi.org/10.1021/ACS.IECR.7B00042

[29] M. Schubert, J. W. Regler, F. Vogel, *J. Supercrit. Fluids* **2010**, *52 (1)*, 99–112. DOI: https://doi.org/10.1016/J.SUPFLU.2009.10.002

[30] J. B. Müller, F. Vogel, *J. Supercrit. Fluids* **2012**, *70*, 126–136. DOI: https://doi.org/10.1016/J.SUPFLU.2012.06.016

[31] N. Boukis, I. Katharina Stoll, *Processes* **2021**, *9 (3)*, 1–17. DOI: https://doi.org/10.3390/pr9030455

[32] P. Azadi, R. Farnood, *Int. J. Hydrogen Energy* **2011**, *36 (16)*, 9529–9541. DOI: https://doi.org/10.1016/J.IJHYDENE.2011.05.081

[33] S. D. Angeli, G. Monteleone, A. Giaconia, A. A. Lemonidou, *Int. J. Hydrogen Energy* **2014**, *39 (5)*, 1979–1997. DOI: https://doi.org/10.1016/j.ijhydene.2013.12.001

[34] L. Chen, Z. Qi, S. Zhang, J. Su, G. A. Somorjai, *Catalysts* **2020**, *10 (8)*, 858. DOI: https://doi.org/10.3390/catal10080858

[35] U. S. Mohanty, M. Ali, M. R. Azhar, A. Al-Yaseri, A. Keshavarz, S. Iglauer, *Int. J. Hydrogen Energy* **2021**, *46 (65)*, 32809–32845. DOI: https://doi.org/10.1016/J.IJHYDENE.2021.07.097

 © 2023 The Authors. ChemBioEng Reviews published by Wiley-VCH GmbH

21969744, 0, Downloaded from https://onlinelibrary.wiley.com/doi/10.1002/cben.202300007 by Karlsruher Institution F. Technologie, Wiley Online Library on [26/07/2023]. See the Terms and Conditions (https://onlinelibrary.wiley.com/terms-and-conditions) on Wiley Online Library for rules of use; OA articles are governed by the applicable Creative Commons License

[36] H. Zhang, Z. Sun, Y. H. Hu, *Renewable Sustainable Energy Rev.* **2021**, *149*, 111330. DOI: https://doi.org/10.1016/j.rser.2021.111330

[37] B. Abdullah, N. A. Abd Ghani, D. V. N. Vo, *J. Cleaner Prod.* **2017**, *162*, 170–185. DOI: https://doi.org/10.1016/j.jclepro.2017.05.176

[38] T. L. Levalley, A. R. Richard, M. Fan, *Int. J. Hydrogen Energy* **2014**, *39 (30)*, 16983–17000. DOI: https://doi.org/10.1016/j.ijhydene.2014.08.041

[39] X. Zhao, B. Joseph, J. Kuhn, S. Ozcan, *iScience* **2020**, *23 (5)*, 101082. DOI: https://doi.org/10.1016/j.isci.2020.101082

[40] G. Nahar, D. Mote, V. Dupont, *Renewable Sustainable Energy Rev.* **2017**, *76*, 1032–1052. DOI: https://doi.org/10.1016/j.rser.2017.02.031

[41] E. Meloni, M. Martino, V. Palma, *Catalysts* **2020**, *10 (3)*, 352. DOI: https://doi.org/10.3390/catal10030352

[42] X. Song, X. Chen, L. Sun, K. Li, X. Sun, C. Wang, P. Ning, *Chem. Eng. J.* **2020**, *399*, 125764. DOI: https://doi.org/10.1016/J.CEJ.2020.125764

[43] K. Aasberg-Petersen, I. Dybkjær, C. V. Ovesen, N. C. Schjødt, J. Sehested, S. G. Thomsen, *J. Nat. Gas Sci. Eng.* **2011**, *3 (2)*, 423–459. DOI: https://doi.org/10.1016/j.jngse.2011.03.004

[44] V. Marcantonio, M. De Falco, M. Capocelli, E. Bocci, A. Colantoni, M. Villarini, *Int. J. Hydrogen Energy* **2019**, *44 (21)*, 10350–10360. DOI: https://doi.org/10.1016/j.ijhydene.2019.02.121

[45] C. Bartholomew, *Encyclopedia of Catalysis*, John Wiley & Sons, New York **2002**. DOI: https://doi.org/10.1002/0471227617.EOC045

[46] G. Peng, C. Ludwig, F. Vogel, *Appl. Catal., B* **2017**, *202*, 262–268. DOI: https://doi.org/10.1016/J.APCATB.2016.09.011

[47] J. A. Okolie, R. Rana, S. Nanda, A. K. Dalai, J. A. Kozinski, *Sustainable Energy Fuels* **2019**, *3 (3)*, 578–598. DOI: https://doi.org/10.1039/C8SE00565F

[48] S. Li, L. Guo, *Int. J. Hydrogen Energy* **2019**, *44 (30)*, 15842–15852. DOI: https://doi.org/10.1016/j.ijhydene.2018.08.205

[49] M. D. Argyle, C. H. Bartholomew, *Catalysts* **2015**, *5 (1)*, 145–269. DOI: https://doi.org/10.3390/CATAL5010145

[50] S. M. Hashemnejad, M. Parvari, *Chin. J. Catal.* **2011**, *32 (1–2)*, 273–279. DOI: https://doi.org/10.1016/S1872-2067(10)60175-1

[51] M. Marafi, A. Stanislaus, *Resour. Conserv. Recycl.* **2008**, *52 (6)*, 859–873. DOI: https://doi.org/10.1016/j.resconrec.2008.02.004

[52] S. Kolbadinejad, A. Ghaemi, *Case Stud. Chem. Environ. Eng.* **2023**, *7*, 100327. DOI: https://doi.org/10.1016/J.CSCEE.2023.100327

[53] I. P. Eliopoulos, G. Eliopoulos, T. Sfendoni, M. Economou-Eliopoulos, *Minerals* **2022**, *12 (7)*, 917. DOI: https://doi.org/10.3390/MIN12070917

[54] R. E. Demirdögen, F. M. Emen, *J. Nat. Sci. Technol.* **2023**, *1 (1)*, 151–165. DOI: https://doi.org/10.5281/zenodo.7384225

[55] M. Dreher, M. Steib, M. Nachtegaal, J. Wambach, F. Vogel, *ChemCatChem* **2014**, *6 (2)*, 626–633. DOI: https://doi.org/10.1002/CCTC.201300791

[56] P. Azadi, E. Afif, F. Azadi, R. Farnood, *Green Chem.* **2012**, *14 (6)*, 1766–1777. DOI: https://doi.org/10.1039/c2gc16378k

[57] J. A. Okolie, A. Mukherjee, S. Nanda, A. K. Dalai, J. A. Kozinski, *Ind. Eng. Chem. Res.* **2021**, *60 (16)*, 5770–5782. DOI: https://doi.org/10.1021/acs.iecr.0c06177

[58] K. Kang, R. Azargohar, A. K. Dalai, H. Wang, *Int. J. Energy Res.* **2017**, *41 (13)*, 1835–1846. DOI: https://doi.org/10.1002/ER.3739

[59] S. Li, L. Guo, *Int. J. Hydrogen Energy* **2019**, 15842–15852. DOI: https://doi.org/10.1016/j.ijhydene.2018.08.205

[60] Q. Guan, S. Chen, Y. Chen, J. Gu, B. Li, R. Miao, Q. Chen, P. Ning, *Int. J. Hydrogen Energy* **2017**, *42 (10)*, 6511–6518. DOI: https://doi.org/10.1016/j.ijhydene.2016.11.191

[61] S. Li, Y. Lu, L. Guo, X. Zhang, *Int. J. Hydrogen Energy* **2011**, *36 (22)*, 14391–14400. DOI: https://doi.org/10.1016/j.ijhydene.2011.07.144

[62] J. Sun, L. Xu, G. Hua Dong, S. Nanda, H. Li, Z. Fang, J. A. Kozinski, A. K. Dalai, *J. Supercrit. Fluids* **2020**, *162*, 2–11. DOI: https://doi.org/10.1016/j.supflu.2020.104863

[63] S. Li, L. Guo, C. Zhu, Y. Lu, *Int. J. Hydrogen Energy* **2013**, *38 (23)*, 9688–9700. DOI: https://doi.org/10.1016/J.IJHYDENE.2013.05.002

[64] K. Kang, R. Azargohar, A. K. Dalai, H. Wang, *Energy Convers. Manage.* **2016**, *117*, 528–537. DOI: https://doi.org/10.1016/j.enconman.2016.03.008

[65] K. Kang, R. Azargohar, A. K. Dalai, H. Wang, *Chem. Eng. J.* **2016**, *283*, 1019–1032. DOI: https://doi.org/10.1016/J.CEJ.2015.08.032

[66] Y. Lu, Y. Zhu, S. Li, X. Zhang, L. Guo, *Biomass Bioenergy* **2014**, *67*, 125–136. DOI: https://doi.org/10.1016/J.BIOMBIOE.2014.04.038

[67] J. Liu, S. Hamid Fauziah, L. Zhong, J. Jiang, G. Zhu, M. Yan, *Fuel* **2022**, *314*, 123042. DOI: https://doi.org/10.1016/j.fuel.2021.123042

[68] B. Hao, W. Ning, D. Xu, Y. Wang, Y. Guo, S. Wang, *Biomass Bioenergy* **2022**, *166*, 106601. DOI: https://doi.org/10.1016/j.biombioe.2022.106601

[69] C. Chen, T. Cang, H. Wibowo, D. Hantoko, E. Kanchanatip, T. Shen, M. Yan, *Int. J. Hydrogen Energy* **2023**. DOI: https://doi.org/10.1016/j.ijhydene.2023.03.290

[70] S. Li, B. Zhu, W. Wang, H. Zhang, Q. Li, *J. Supercrit. Fluids* **2020**, *160*, 104790. DOI: https://doi.org/10.1016/j.supflu.2020.104790

[71] J. A. Onwudili, P. T. Williams, *Appl. Catal., B* **2013**, *132–133*, 70–79. DOI: https://doi.org/10.1016/j.apcatb.2012.11.033

[72] M. Yang, J. Zhang, Y. Guo, *J. Supercrit. Fluids* **2020**, *160*, 104810. DOI: https://doi.org/10.1016/j.supflu.2020.104810

[73] C. Hunston, D. Baudouin, L. Koning, A. Agarwal, O. Kröcher, F. Vogel, *Appl. Catal., B* **2023**, *320*. DOI: https://doi.org/10.1016/j.apcatb.2022.121956

[74] M. Barati, M. Babatabar, A. Tavasoli, A. K. Dalai, U. Das, *Fuel Process. Technol.* **2014**, *123*, 140–148. DOI: https://doi.org/10.1016/j.fuproc.2014.02.005

[75] L. Tiong, M. Komiyama, Y. Uemura, T. T. Nguyen, *J. Supercrit. Fluids* **2016**, *107*, 408–413. DOI: https://doi.org/10.1016/j.supflu.2015.10.009

[76] A. Pei, L. Zhang, B. Jiang, L. Guo, X. Zhang, Y. Lv, H. Jin, *Front. Energy Power Eng. China* **2009**, *3 (4)*, 456–464. DOI: https://doi.org/10.1007/S11708-009-0069-Y

 © 2023 The Authors. ChemBioEng Reviews published by Wiley-VCH GmbH

21963744, 0, Downloaded from https://onlinelibrary.wiley.com/doi/10.1002/cben.202300007 by Karlsruher Institution F. Technologie, Wiley Online Library on [26/07/2023]. See the Terms and Conditions (https://onlinelibrary.wiley.com/terms-and-conditions) on Wiley Online Library for rules of use; OA articles are governed by the applicable Creative Commons License

[77] H. Jin, Y. Lu, L. Guo, X. Zhang, A. Pei, *Adv. Condens. Matter Phys.* **2014**, *2014*, 160565. DOI: https://doi.org/10.1155/2014/160565

[78] Y. Chen, L. Yi, S. Li, J. Yin, H. Jin, *Chem. Eng. J.* **2020**, *388*, 124292. DOI: https://doi.org/10.1016/j.cej.2020.124292

[79] Y. Lu, S. Li, L. Guo, X. Zhang, *Int. J. Hydrogen Energy* **2010**, *35 (13)*, 7161–7168. DOI: https://doi.org/10.1016/j.ijhydene.2009.12.047

[80] N. Ding, R. Azargohar, A. K. Dalai, J. A. Kozinski, *Fuel Process. Technol.* **2014**, *127*, 33–40. DOI: https://doi.org/10.1016/J.FUPROC.2014.05.014

[81] Y. Lu, S. Li, L. Guo, *Fuel* **2013**, *103*, 193–199. DOI: https://doi.org/10.1016/J.FUEL.2012.04.038

[82] Y. Q. Shan, L. X. Yin, O. S. Djandja, Z. C. Wang, P. G. Duan, *Fuel* **2021**, *292*, 120288. DOI: https://doi.org/10.1016/j.fuel.2021.120288

[83] J. Yin, Z. Cheng, L. Guo, S. Li, H. Jin, *Int. J. Hydrogen Energy* **2017**, *42 (7)*, 4642–4650. DOI: https://doi.org/10.1016/J.IJHYDENE.2016.07.065

[84] M. S. Mastuli, M. F. Kasim, A. M. Mahat, N. Asikin-Mijan, S. Sivasangar, Y. H. Taufiq-Yap, *Int. J. Hydrogen Energy* **2020**, *45 (58)*, 33218–33234. DOI: https://doi.org/10.1016/j.ijhydene.2020.09.020

[85] M. S. Mastuli, N. Kamarulzaman, M. F. Kasim, Z. Zainal, Y. Matsumura, Y. H. Taufiq-Yap, *Int. J. Hydrogen Energy* **2019**, *44 (7)*, 3690–3701. DOI: https://doi.org/10.1016/j.ijhydene.2018.12.102

[86] Q. Liu, L. Liao, Z. Liu, X. Dong, *J. Energy Chem.* **2013**, *22 (4)*, 665–670. DOI: https://doi.org/10.1016/S2095-4956(13)60088-1

[87] T. Sato, T. Furusawa, Y. Ishiyama, H. Sugito, Y. Miura, M. Sato, N. Suzuki, N. Itoh, *Ind. Eng. Chem. Res.* **2006**, *45 (2)*, 615–622. DOI: https://doi.org/10.1021/ie0510270

[88] T. Furusawa, T. Sato, M. Saito, Y. Ishiyama, *Appl. Catal., A* **2007**, *327*, 300–310. DOI: https://doi.org/10.1016/j.apcata.2007.05.036

[89] B. Yan, J. Wu, C. Xie, F. He, C. Wei, *J. Supercrit. Fluids* **2009**, *50 (2)*, 155–161. DOI: https://doi.org/10.1016/j.supflu.2009.04.015

[90] B. Zhu, S. Li, W. Wang, H. Zhang, *Int. J. Hydrogen Energy* **2019**, *44 (59)*, 30917–30926. DOI: https://doi.org/10.1016/j.ijhydene.2019.10.044

[91] S. Li, P. E. Savage, L. Guo, *J. Supercrit. Fluids* **2019**, *148*, 137–147. DOI: https://doi.org/10.1016/j.supflu.2019.02.028

[92] J. Kou, L. Yi, G. Li, K. Cheng, R. Wang, D. Zhang, H. Jin, L. Guo, *Int. J. Hydrogen Energy* **2021**, *46 (24)*, 12874–12885. DOI: https://doi.org/10.1016/j.ijhydene.2021.01.082

[93] J. Huang, X. Lian, L. Wang, C. Zhu, H. Jin, R. Wang, *Int. J. Hydrogen Energy* **2017**, *42 (7)*, 4613–4625. DOI: https://doi.org/10.1016/J.IJHYDENE.2016.10.012

[94] I. G. Lee, A. Nowacka, C. H. Yuan, S. J. Park, J. B. Yang, *Int. J. Hydrogen Energy* **2015**, *40 (36)*, 12078–12087. DOI: https://doi.org/10.1016/J.IJHYDENE.2015.07.112

[95] A. Sina, T. Yumak, V. Balci, A. Kruse, *J. Supercrit. Fluids* **2011**, *56 (2)*, 179–185. DOI: https://doi.org/10.1016/J.SUPFLU.2011.01.002

[96] S. Sivasangar, M. S. Mastuli, A. Islam, Y. H. Taufiq-Yap, *RSC Adv.* **2015**, *5 (46)*, 36798–36808. DOI: https://doi.org/10.1039/C5RA03430B

[97] C. Cao, L. Yu, Y. Xie, W. Wei, H. Jin, *Int. J. Hydrogen Energy* **2022**, *47 (14)*, 8716–8728. DOI: https://doi.org/10.1016/j.ijhydene.2021.12.230

[98] H. Jin, X. Zhao, Z. Wu, C. Cao, L. Guo, *J. Exp. Nanosci.* **2017**, *12 (1)*, 72–82. DOI: https://doi.org/10.1080/17458080.2016.1262066

[99] M. Karakaya, S. Keskin, A. K. Avci, *Appl. Catal., A* **2012**, *411–412*, 114–122. DOI: https://doi.org/10.1016/j.apcata.2011.10.028

[100] M. Ambrosetti, D. Bonincontro, R. Balzarotti, A. Beretta, G. Groppi, E. Tronconi, *Catal. Today* **2022**, *387*, 107–118. DOI: https://doi.org/10.1016/j.cattod.2021.06.003

[101] R. Zapf, R. Thiele, M. Wichert, M. O'Connell, A. Ziogas, G. Kolb, *Catal. Commun.* **2013**, *41*, 140–145. DOI: https://doi.org/10.1016/j.catcom.2013.07.018

[102] Z. O. Malaibari, E. Croiset, A. Amin, W. Epling, *Appl. Catal., A* **2015**, *490*, 80–92. DOI: https://doi.org/10.1016/j.apcata.2014.11.002

[103] M. S. P. Sudhakaran, M. M. Hossain, G. Gnanasekaran, Y. S. Mok, *Catalysts* **2019**, *9 (1)*, 68. DOI: https://doi.org/10.3390/catal9010068

[104] E. V. Matus, I. Z. Ismagilov, S. A. Yashnik, V. A. Ushakov, I. P. Prosvirin, M. A. Kerzhentsev, Z. R. Ismagilov, *Int. J. Hydrogen Energy* **2020**, *45 (58)*, 33352–33369. DOI: https://doi.org/10.1016/j.ijhydene.2020.09.011

[105] T. Borowiecki, A. Denis, W. Gac, R. Dziembaj, Z. Piwowarska, M. Drozdek, *Appl. Catal., A* **2004**, *274 (1–2)*, 259–267. DOI: https://doi.org/10.1016/J.APCATA.2004.07.009

[106] L. Yao, M. E. Galvez, C. Hu, P. Da Costa, *Int. J. Hydrogen Energy* **2017**, *42 (37)*, 23500–23507. DOI: https://doi.org/10.1016/j.ijhydene.2017.03.208

[107] N. V. Parizotto, K. O. Rocha, S. Damyanova, F. B. Passos, D. Zanchet, C. M. P. Marques, J. M. C. Bueno, *Appl. Catal., A* **2007**, *330 (1–2)*, 12–22. DOI: https://doi.org/10.1016/j.apcata.2007.06.022

[108] H. Wang, D. W. Blaylock, A. H. Dam, S. E. Liland, K. R. Rout, Y. A. Zhu, W. H. Green, A. Holmen, D. Chen, *Catal. Sci. Technol.* **2017**, *7 (8)*, 1713–1725. DOI: https://doi.org/10.1039/c7cy00101k

[109] A. H. Dam, H. Wang, R. Dehghan-Niri, X. Yu, J. C. Walmsley, A. Holmen, J. Yang, D. Chen, *ChemCatChem* **2019**, *11 (15)*, 3401–3412. DOI: https://doi.org/10.1002/cctc.201900679

[110] I. R. Azevedo, A. A. A. da Silva, Y. T. Xing, R. C. Rabelo-Neto, N. T. J. Luchters, J. C. Q. Fletcher, F. B. Noronha, L. V. Mattos, *Int. J. Hydrogen Energy* **2022**, *47 (35)*, 15624–15640. DOI: https://doi.org/10.1016/j.ijhydene.2022.03.067

[111] W. Zeng, L. Li, M. Song, X. Wu, G. Li, C. Hu, *Int. J. Hydrogen Energy* **2023**, *48 (16)*, 6358–6369. DOI: https://doi.org/10.1016/J.IJHYDENE.2022.05.088

[112] J. Xu, W. Zhou, Z. Li, J. Wang, J. Ma, *Int. J. Hydrogen Energy* **2010**, *35 (23)*, 13013–13020. DOI: https://doi.org/10.1016/j.ijhydene.2010.04.075

[113] S. Zolghadri, B. Honarvar, M. R. Rahimpour, *Fuel* **2023**, *335*, 127005. DOI: https://doi.org/10.1016/j.fuel.2022.127005

[114] H. Ay, D. Üner, *Appl. Catal., B* **2015**, *179*, 128–138. DOI: https://doi.org/10.1016/j.apcatb.2015.05.013

 © 2023 The Authors. ChemBioEng Reviews published by Wiley-VCH GmbH

21969744, 0, Downloaded from https://onlinelibrary.wiley.com/doi/10.1002/cben.202300007 by Karlsruher Institution F. Technologie, Wiley Online Library on [26/07/2023]. See the Terms and Conditions (https://onlinelibrary.wiley.com/terms-and-conditions) on Wiley Online Library for rules of use; OA articles are governed by the applicable Creative Commons License

[115] F. Zarei-Jelyani, F. Salahi, M. Farsi, M. Reza Rahimpour, *Fuel* **2022**, *324*, 124785. DOI: https://doi.org/10.1016/j.fuel.2022.124785
[116] H. Khosravani, M. Meshksar, M. Koohi-Saadi, K. Taghadom, M. R. Rahimpour, *J. Energy Inst.* **2023**, *108*, 101203. DOI: https://doi.org/10.1016/j.joei.2023.101203
[117] M. Meshksar, M. Farsi, M. R. Rahimpour, *J. Energy Inst.* **2022**, *105*, 342–354. DOI: https://doi.org/10.1016/j.joei.2022.10.006
[118] K. Großmann, T. Dellermann, M. Dillig, J. Karl, *Int. J. Hydrogen Energy* **2017**, *42 (16)*, 11150–11158. DOI: https://doi.org/10.1016/j.ijhydene.2017.02.073
[119] C. E. Tuna, J. L. Silveira, M. E. da Silva, R. M. Boloy, L. B. Braga, N. P. Pérez, *Int. J. Hydrogen Energy* **2018**, *3*, 2108–2120. DOI: https://doi.org/10.1016/j.ijhydene.2017.12.008
[120] N. Zhang, X. Chen, B. Chu, C. Cao, Y. Jin, Y. Cheng, *Chem. Eng. Process. Process Intensif.* **2017**, *118*, 19–25. DOI: https://doi.org/10.1016/j.cep.2017.04.015
[121] L. Zhang, X. Wang, B. Tan, U. S. Ozkan, *J. Mol. Catal. A: Chem.* **2009**, *297 (1–2)*, 26–34. DOI: https://doi.org/10.1016/j.molcata.2008.09.011
[122] H. S. Roh, I. H. Eum, D. W. Jeong, *Renewable Energy* **2012**, *42*, 212–216. DOI: https://doi.org/10.1016/j.renene.2011.08.013
[123] M. A. Goula, N. D. Charisiou, G. Siakavelas, L. Tzounis, I. Tsiaoussis, P. Panagiotopoulou, G. Goula, I. V. Yentekakis, *Int. J. Hydrogen Energy* **2017**, *42 (19)*, 13724–13740. DOI: https://doi.org/10.1016/j.ijhydene.2016.11.196
[124] M. M. Makri, M. A. Vasiliades, K. C. Petallidou, A. M. Efstathiou, *Catal. Today* **2016**, *259*, 150–164. DOI: https://doi.org/10.1016/j.cattod.2015.06.010
[125] M. Dan, M. Mihet, A. R. Biris, P. Marginean, V. Almasan, G. Borodi, F. Watanabe, A. S. Biris, M. D. Lazar, *React. Kinet. Mech. Catal.* **2012**, *105 (1)*, 173–193. DOI: https://doi.org/10.1007/s11144-011-0406-0
[126] B. Li, S. Zhang, *Int. J. Hydrogen Energy* **2013**, *38 (33)*, 14250–14260. DOI: https://doi.org/10.1016/J.IJHYDENE.2013.08.105
[127] V. Shanmugam, R. Zapf, V. Hessel, H. Pennemann, G. Kolb, *Appl. Catal., B* **2018**, *226*, 403–411. DOI: https://doi.org/10.1016/j.apcatb.2017.12.062
[128] V. Shanmugam, R. Zapf, S. Neuberg, V. Hessel, G. Kolb, *Appl. Catal., B* **2017**, *203*, 859–869. DOI: https://doi.org/10.1016/J.APCATB.2016.10.075
[129] J. A. Santander, G. M. Tonetto, M. N. Pedernera, E. López, *Int. J. Hydrogen Energy* **2017**, *42 (15)*, 9482–9492. DOI: https://doi.org/10.1016/j.ijhydene.2017.03.169
[130] Z. W. Liu, K. W. Jun, H. S. Roh, S. E. Park, *J. Power Sources* **2002**, *111 (2)*, 283–287. DOI: https://doi.org/10.1016/S0378-7753(02)00317-8
[131] M. J. Park, J. H. Kim, Y. H. Lee, H. M. Kim, D. W. Jeong, *Int. J. Hydrogen Energy* **2020**, *45 (55)*, 30188–30200. DOI: https://doi.org/10.1016/j.ijhydene.2020.08.027
[132] S. D. Angeli, L. Turchetti, G. Monteleone, A. A. Lemonidou, *Appl. Catal., B* **2016**, *181*, 34–46. DOI: https://doi.org/10.1016/j.apcatb.2015.07.039
[133] X. Wang, R. J. Gorte, *Appl. Catal., A* **2002**, *224 (1–2)*, 209–218. DOI: https://doi.org/10.1016/S0926-860X(01)00783-9
[134] P. S. Roy, J. Song, K. Kim, J.-M. Kim, C. S. Park, A. S. K. Raju, *J. Ind. Eng. Chem.* **2018**, *62*, 120–129. DOI: https://doi.org/10.1016/j.jiec.2017.12.050
[135] S. Sepehri, M. Rezaei, *Int. J. Hydrogen Energy* **2017**, *42 (16)*, 11130–11138. DOI: https://doi.org/10.1016/j.ijhydene.2017.01.096
[136] X. Yang, J. Da, H. Yu, H. Wang, *Fuel* **2016**, *179*, 353–361. DOI: https://doi.org/10.1016/j.fuel.2016.03.104
[137] S. Choi, J. Bae, S. Lee, J. Oh, S. P. Katikaneni, *Chem. Eng. Sci.* **2017**, *168*, 15–22. DOI: https://doi.org/10.1016/j.ces.2017.04.033
[138] I. Luisetto, S. Tuti, C. Battocchio, S. Lo Mastro, A. Sodo, *Appl. Catal., A* **2015**, *500*, 12–22. DOI: https://doi.org/10.1016/j.apcata.2015.05.004
[139] Z. Bao, Y. Lu, J. Han, Y. Li, F. Yu, *Appl. Catal., A* **2015**, *491*, 116–126. DOI: https://doi.org/10.1016/j.apcata.2014.12.005
[140] K. Jabbour, P. Massiani, A. Davidson, S. Casale, N. El Hassan, *Appl. Catal., B* **2017**, *201*, 527–542. DOI: https://doi.org/10.1016/j.apcatb.2016.08.009
[141] K. M. Kang, I. W. Shim, H. Y. Kwak, *Fuel Process. Technol.* **2012**, *93 (1)*, 105–114. DOI: https://doi.org/10.1016/j.fuproc.2011.09.022
[142] O. Sidjabat, D. L. Trimm, *Top. Catal.* **2000**, *11–12 (1–4)*, 279–282. DOI: https://doi.org/10.1023/A:1027212301077
[143] R. Lødeng, De Chen, K. O. Christensen, H. S. Andersen, M. Rønnekleiv, A. Holmen, *ACS Div. Fuel Chem. Prep.* **2003**, *48 (1)*, 372–373.
[144] S. M. Mousavi, F. Meshkani, M. Rezaei, *J. Environ. Chem. Eng.* **2017**, *5 (6)*, 5493–5500. DOI: https://doi.org/10.1016/j.jece.2017.10.020
[145] R. P. Borges, L. G. Moura, S. Kanitkar, J. J. Spivey, F. B. Noronha, C. E. Hori, *Catal. Today* **2021**, *381*, 3–12. DOI: https://doi.org/10.1016/j.cattod.2021.06.024
[146] U. Rodemerck, M. Schneider, D. Linke, *Catal. Commun.* **2017**, *102*, 98–102. DOI: https://doi.org/10.1016/j.catcom.2017.08.031
[147] Y. Kathiraser, Z. Wang, M. L. Ang, L. Mo, Z. Li, U. Oemar, S. Kawi, *J. CO2 Util.* **2017**, *19*, 284–295. DOI: https://doi.org/10.1016/j.jcou.2017.03.018
[148] G. Garbarino, F. Pugliese, T. Cavattoni, G. Busca, P. Costamagna, *Energies* **2020**, *13 (11)*, 2792. DOI: https://doi.org/10.3390/en13112792
[149] S. Mhadmhan, P. Natewong, N. Prasongthum, C. Samart, P. Reubroycharoen, *Catalysts* **2018**, *8 (8)*, 1–18. DOI: https://doi.org/10.3390/catal8080319
[150] V. Palma, M. Martino, E. Meloni, A. Ricca, *Int. J. Hydrogen Energy* **2017**, *42 (3)*, 1629–1638. DOI: https://doi.org/10.1016/j.ijhydene.2016.06.162
[151] A. Ricca, V. Palma, M. Martino, E. Meloni, *Fuel* **2017**, *198*, 175–182. DOI: https://doi.org/10.1016/j.fuel.2016.11.006
[152] A. J. Vizcaíno, A. Carrero, J. A. Calles, *Fuel Process. Technol.* **2016**, *146*, 99–109. DOI: https://doi.org/10.1016/j.fuproc.2016.02.020
[153] Z. Taherian, A. Khataee, Y. Orooji, *Renewable Sustainable Energy Rev.* **2020**, *134*, 110130. DOI: https://doi.org/10.1016/j.rser.2020.110130
[154] N. Habibi, Y. Wang, H. Arandiyan, M. Rezaei, *Int. J. Hydrogen Energy* **2017**, *42 (38)*, 24159–24168. DOI: https://doi.org/10.1016/j.ijhydene.2017.07.222

 © 2023 The Authors. ChemBioEng Reviews published by Wiley-VCH GmbH

21969744, 0, Downloaded from https://onlinelibrary.wiley.com/doi/10.1002/cben.202300007 by Karlsruher Institution F. Technologie, Wiley Online Library on [26/07/2023]. See the Terms and Conditions (https://onlinelibrary.wiley.com/terms-and-conditions) on Wiley Online Library for rules of use; OA articles are governed by the applicable Creative Commons License

[155] Y. Khani, Z. Shariatinia, F. Bahadoran, *Chem. Eng. J.* **2016**, *299*, 353–366. DOI: https://doi.org/10.1016/j.cej.2016.04.108
[156] V. K. Jaiswar, S. Katheria, G. Deo, D. Kunzru, *Int. J. Hydrogen Energy* **2017**, *42 (30)*, 18968–18976. DOI: https://doi.org/10.1016/j.ijhydene.2017.06.096
[157] A. Z. Senseni, M. Rezaei, F. Meshkani, *Chem. Eng. Res. Des.* **2017**, *123 (3)*, 360–366. DOI: https://doi.org/10.1016/j.cherd.2017.05.020
[158] K. Y. Koo, S. H. Lee, U. H. Jung, H. S. Roh, W. L. Yoon, *Fuel Process. Technol.* **2014**, *119*, 151–157. DOI: https://doi.org/10.1016/j.fuproc.2013.11.005
[159] A. Movasati, S. M. Alavi, G. Mazloom, *Int. J. Hydrogen Energy* **2017**, *42 (26)*, 16436–16448. DOI: https://doi.org/10.1016/j.ijhydene.2017.05.199
[160] D. H. Kim, J. R. Youn, J. C. Seo, S. B. Kim, M. J. Kim, K. Lee, *Catal. Today* **2023**, *411–412*, 113910. DOI: https://doi.org/10.1016/j.cattod.2022.09.016
[161] G. P. Szijjártó, Z. Pászti, I. Sajó, A. Erdohelyi, G. Radnóczi, A. Tompos, *J. Catal.* **2013**, *305*, 290–306. DOI: https://doi.org/10.1016/J.JCAT.2013.05.036
[162] C. Wang, N. Sun, N. Zhao, W. Wei, Y. Sun, C. Sun, H. Liu, C. E. Snape, *Fuel* **2015**, *143*, 527–535. DOI: https://doi.org/10.1016/j.fuel.2014.11.097
[163] K. Lertwittayanon, W. Youravong, W. J. Lau, *Int. J. Hydrogen Energy* **2017**, *42 (47)*, 28254–28265. DOI: https://doi.org/10.1016/j.ijhydene.2017.09.030
[164] N. D. Charisiou, A. Baklavaridis, V. G. Papadakis, M. A. Goula, *Waste Biomass Valorization* **2016**, *7 (4)*, 725–736. DOI: https://doi.org/10.1007/s12649-016-9627-9
[165] M. Mundhwa, C. P. Thurgood, *Fuel Process. Technol.* **2017**, *168*, 27–39. DOI: https://doi.org/10.1016/J.FUPROC.2017.08.031
[166] R. Patel, A. H. Fakeeha, S. O. Kasim, M. L. Sofiu, A. A. Ibrahim, A. E. Abasaeed, R. Kumar, A. S. Al-Fatesh, *Mol. Catal.* **2021**, *510*, 111676. DOI: https://doi.org/10.1016/J.MCAT.2021.111676
[167] Z. L. Zhang, X. E. Verykios, *Catal. Today* **1994**, *21 (2–3)*, 589–595. DOI: https://doi.org/10.1016/0920-5861(94)80183-5
[168] M. A. Muñoz, J. J. Calvino, J. M. Rodríguez-Izquierdo, G. Blanco, D. C. Arias, J. A. Pérez-Omil, J. C. Hernández-Garrido, J. M. González-Leal, M. A. Cauqui, M. P. Yeste, *Appl. Surf. Sci.* **2017**, *426*, 864–873. DOI: https://doi.org/10.1016/J.APSUSC.2017.07.210
[169] A. H. Fakeeha, A. S. Al Fatesh, A. A. Ibrahim, A. N. Kurdi, A. E. Abasaeed, *ACS Omega* **2021**, *6 (2)*, 1280–1288. DOI: https://doi.org/10.1021/acsomega.0c04731
[170] K. Świrk, M. E. Gálvez, M. Motak, T. Grzybek, M. Rønning, P. Da Costa, *J. CO2 Util.* **2018**, 247–258. DOI: https://doi.org/10.1016/j.jcou.2018.08.004
[171] K. Świrk Da Costa, H. Zhang, S. Li, Y. Chen, M. Rønning, M. Motak, T. Grzybek, P. Da Costa, *Catal. Today* **2021**, *366*, 103–113. DOI: https://doi.org/10.1016/j.cattod.2020.03.032
[172] K. Świrk, M. Rønning, M. Motak, P. Beaunier, P. Da Costa, T. Grzybek, *Catalysts* **2019**, *9 (1)*, 56. DOI: https://doi.org/10.3390/catal9010056
[173] Y. Wang, L. Li, Y. Wang, P. Da Costa, C. Hu, *Catalysts* **2019**, *9 (12)*, 1–13. DOI: https://doi.org/10.3390/catal9121055
[174] S. Damyanova, I. Shtereva, B. Pawelec, L. Mihaylov, J. L. G. Fierro, *Appl. Catal., B* **2020**, *278*, 119335. DOI: https://doi.org/10.1016/J.APCATB.2020.119335
[175] B. W. Kwon, G. S. Kim, J. H. Oh, S. C. Jang, S. P. Yoon, J. Han, S. W. Nam, H. C. Ham, *Energy Procedia* **2017**, *105*, 1942–1947. DOI: https://doi.org/10.1016/j.egypro.2017.03.564
[176] M. Karaismailoglu, H. E. Figen, S. Z. Baykara, *Int. J. Hydrogen Energy* **2019**, *44 (20)*, 9922–9929. DOI: https://doi.org/10.1016/J.IJHYDENE.2018.12.214
[177] X. Fang, X. Zhang, Y. Guo, M. Chen, W. Liu, X. Xu, H. Peng, Z. Gao, X. Wang, C. Li, *Int. J. Hydrogen Energy* **2016**, *41 (26)*, 11141–11153. DOI: https://doi.org/10.1016/j.ijhydene.2016.04.038
[178] K. Hbaieb, K. K. A. Rashid, F. Kooli, *Int. J. Hydrogen Energy* **2017**, *42 (8)*, 5114–5124. DOI: https://doi.org/10.1016/j.ijhydene.2016.11.127

 © 2023 The Authors. ChemBioEng Reviews published by Wiley-VCH GmbH

21969744, 0, Downloaded from https://onlinelibrary.wiley.com/doi/10.1002/cben.202300007 by Karlsruher Institution F. Technologie, Wiley Online Library on [26/07/2023]. See the Terms and Conditions (https://onlinelibrary.wiley.com/terms-and-conditions) on Wiley Online Library for rules of use; OA articles are governed by the applicable Creative Commons License

Biomass gasification with supercritical water is a sustainable method of hydrogen production. Recent research on this topic is reviewed, demonstrating that this process produces not only hydrogen gas but also a mixture of hydrocarbons, which bind a part of it in the H–C bonds. An innovative process for upgrading the gaseous product while focusing on the most suitable catalysts is proposed.

Catalytic Biomass Gasification in Supercritical Water and Product Gas Upgrading

Athanasios A. Vadarlis*, Sofia D. Angeli, Angeliki A. Lemonidou, Nikolaos Boukis, Jörg Sauer

ChemBioEng Rev. **2023**, *10 (X)*, **XXX** ··· **XXX**

DOI: 10.1002/cben.202300007

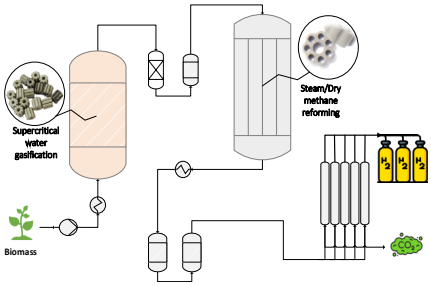

 © 2023 The Authors. ChemBioEng Reviews published by Wiley-VCH GmbH

21963744, 0, Downloaded from https://onlinelibrary.wiley.com/doi/10.1002/cben.202300007 by Karlsruher Institution F. Technologie, Wiley Online Library on [26/07/2023]. See the Terms and Conditions (https://onlinelibrary.wiley.com/terms-and-conditions) on Wiley Online Library for rules of use; OA articles are governed by the applicable Creative Commons License